Chem Soc Rev

REVIEW ARTICLE

View Article Online
View Journal

Cite this: DOI: 10.1039/c3cs60276a

Controlling morphology and porosity to improve performance of molecularly imprinted sol–gel silica

Jennifer E. Lofgreen and Geoffrey A. Ozin*

Received 26th July 2013

DOI: 10.1039/c3cs60276a

www.rsc.org/csr

The wealth of molecular precursors for organic and inorganic polymers has resulted in an incredible volume of molecular imprinting literature. The vast majority of reports deal with organic polymer systems, and molecular imprinting in silica can still be considered a small niche in the field. In this review, we present key concepts of molecular imprinting, sol–gel processing, and the synthesis of templated mesoporous silica. We take a small fraction of the literature and use it to understand the ways in which molecular imprinting in siliceous materials of controlled morphology has achieved success in the past fifteen years. Using selected case studies rather than a comprehensive review of the entire field, our goal is to illustrate the key aspects of imprinted silica-based materials as demonstrated by judiciously controlled systems, looking first at control on the micrometre scale in bulk phase materials, and then on the nanometre scale in templated mesoporous materials.

Introduction

The field of molecular imprinting encompasses a vast array of methods, materials, and applications. The number of combinations that can produce a molecularly imprinted polymer (MIP) is essentially infinite, and the pursuit of optimized systems has resulted in thousands of publications. The starting point for new research in molecular imprinting can either be a target molecule or a desired matrix. In this review, the relatively small field of molecular imprinting in silica (small only relative to that of organic MIPs) will be discussed using a selection of

Department of Chemistry, University of Toronto, 80 St. George Street, Toronto, ON, M5S 3H6, Canada. E-mail: gozin@chem.utoronto.ca

Jennifer E. Lofgreen

Jennifer Lofgreen completed her Honours BSc in Materials Chemistry at McGill University and earned her PhD in Chemistry as a member of the Ozin group at the University of Toronto in 2013. Her doctoral research focused on molecular imprinting in templated mesoporous organosilica materials, with particular emphasis on the influence of controlled porosity on the performance of imprinted materials. An award-winning conference presenter, Jennifer is especially interested in promoting the development of communication excellence in the natural sciences and engineering. Currently, she is a communication instructor at the University of Toronto in the Faculty of Applied Science and Engineering and in the School of Graduate Studies' Office for English Language and Writing Support.

Geoffrey A. Ozin

Geoffrey Ozin studied at King's College London and Oriel College Oxford University, before completing an ICI Postdoctoral Fellowship at Southampton University. Currently he is the Tier 1 Canada Research Chair in Materials Chemistry and Nanochemistry, Distinguished University Professor at the University of Toronto, and a Founding Fellow of the Nanoscience Team at the Canadian Institute for Advanced Research. Internationally currently he is Distinguished Professor at Karlsruhe Institute of Technology (KIT). Over a four decade career he has made innovative and transformative fundamental scientific and technological advances in the field of nanochemistry, a chemistry approach to nanocrystals and nanowires, nanoporous materials, nanophotonic crystals and nanomotors that led to nanoscale constructs capable of controlling electrons, photons, phonons and motion in unprecedented ways.

illustrative examples selected from the literature. A number of excellent reviews give exceptionally thorough accounts of imprinting in silica up to 2012.[1–6] Instead of providing a comprehensive review of the field, the goal here is to examine the ways that researchers have approached molecular imprinting in silica with controlled morphologies. First, a definition and brief history of molecular imprinting will position silica as a matrix material. Next, the key concepts of molecular imprinting and sol–gel processing will establish a fundamental understanding of the field. Finally, selected cases will present the variety of approaches used recently (that is, in the last fifteen years) to produce imprinted silica materials, and discuss in each case the particular advantages and/or challenges of the given system (including the imprinting method and material morphology). In particular, we will highlight the use of templated controlled porosity as a deliberate morphological choice in imprinted silica, and discuss its impact on material performance.

An overview of molecular imprinting

A definition

Molecular imprinting is defined as the assembly of a cross-linked polymer matrix around an imprint molecule that is held in place, either covalently or noncovalently, by judiciously chosen functional monomers (Fig. 1). The removal of the imprint molecule yields an imprint cavity of a specific size and shape. The surface of the imprint cavity contains functional groups that are able to interact, either covalently or non-covalently, with complementary moieties on an appropriately sized target molecule. The target molecule may be, but is not always, the same as the imprint molecule. The matrix that surrounds the imprint molecule is made up of a cross-linked polymer, formed from cross-linking monomers. The functional monomers (there may be one or many, of one type or several) that hold the imprint molecule in place are compatible with the cross-linker but contain a distinct functional group that interacts preferentially or forms a bond with the imprint molecule. In the final MIP, the imprint cavity remains when the imprint molecule is removed, and is able to interact with a target molecule through any combination of size, shape, and functional group matching.

The goal of molecular imprinting is selectivity, either for a specific species or for a molecular fragment. Either way, the applications for MIPs are grouped into two main categories: sensing and separation. Depending on the intended application, the approach to imprinting and preparation of the MIP will change.

A brief history, mostly in silica

The field of molecular imprinting is drawing close to it centennial. The number of publications related to molecular imprinting published annually has risen steadily in the past three decades (Fig. 2),[7] and a search of the concept "molecular imprint" in Scifinder returns more than 12 000 references. Review articles number in the dozens.[8–12] As this field continues to grow, a look back at the earliest discoveries gives perspective and illuminates the crucial role that interdisciplinary chemistry plays in molecular imprinting. This brief history is by no means meant to be exhaustive, as an excellent review has already provided an exceptionally thorough account of the development of the field.[9]

In 1931, Soviet chemist M. K. Polyakov reported that silica particles prepared from sodium silicate in the presence of organic additives (benzene, toluene, or xylene) demonstrated an increased uptake capacity for the associated additive over the other two structural analogues.[13] Because the explanation for this preferential uptake was related to a templating effect from the additive used, this report is the earliest example of the concept of molecular imprinting to be found in the literature. At that time, researchers like Linus Pauling were pondering the origin of the selectivity of antibodies. Pauling's theory was that antigens templated the formation of antibodies, and created structures complementary to themselves.[14] In essence, he was arguing for bio-imprinting, and was the first in his field to do so. Published in 1942, experimental results of the preparation of artificial antibodies using methyl blue dye as the antigen[15] are the earliest known reports of the connection between the biological templating that happens in nature and a synthetic imitation of this process. Like Paul Ehrlich before him,[16]

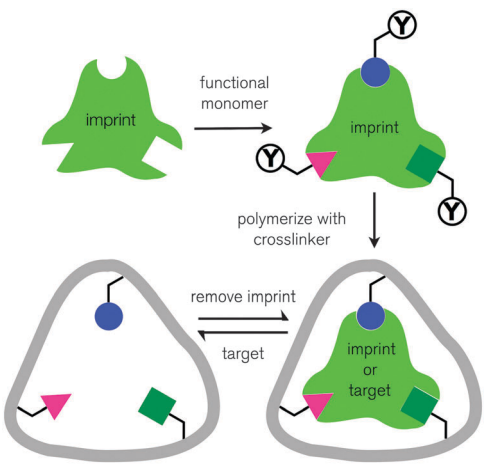

Fig. 1 General process of molecular imprinting.

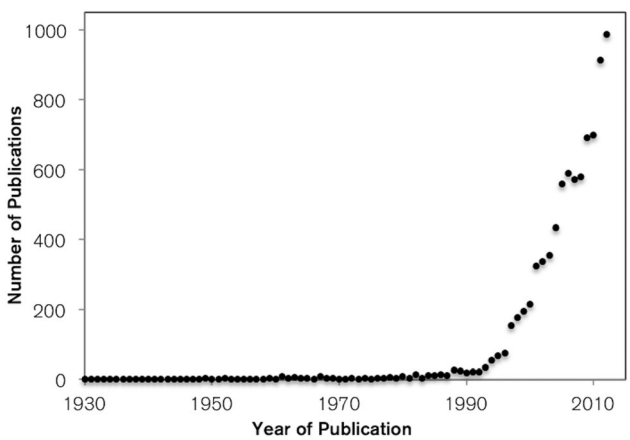

Fig. 2 Number of publications per year in the field of molecular imprinting from 1931 to 2012.[7]

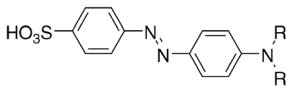

Fig. 3 Structure of alkyl orange dye. R = Me, Et, *n*-Pr, or *n*-Bu.

Pauling drew on Emil Fischer's "lock-and-key" principle of enzyme action to describe the complementarity that also governed antigen–antibody interactions.[17]

Pauling's student, Frank Dickey, published a study some years later in which he extended Pauling's theory of bio-imprinting and the lock-and-key concept backwards to silica,[18] presumably with no knowledge of Polyakov's report almost two decades earlier. Unlike Polyakov, who introduced the chosen organic additive late in the silica gel synthesis, Dickey added alkyl orange dyes to the initial mixture of sodium silicate and glacial acetic acid used to synthesize what he called "specific adsorbents" (Fig. 3). The results of affinity tests for the different dyes pointed to an imprinting effect, particularly in the case of propyl orange. Dickey noted that the results would likely be more pronounced if the dyes differed in structure by more than just the alkyl groups on the tertiary amine. In a later paper, Dickey attempted to explain the mechanism by which a specific adsorbent was created.[19] He suggested that two related processes might be responsible: the first one involved the dye attracting parts of the gel that were still fluid to form an attraction-favouring configuration that becomes part of the final rigid structure; the second relied on the fact that an attraction-favouring configuration that forms spontaneously would likely survive the condensation of the surrounding matrix and inhibit further reaction at that site. This explanation bears a striking resemblance to our current understanding of how molecular imprinting works.

More thorough follow-up work using the same silica and alkyl orange dye system resulted in the first use of the term "imprint" to describe the micropores in the adsorbent created by the dye molecule used.[20] This term and Dickey's proposed mechanism were contested shortly thereafter by Morrison and coworkers at the University of Alberta, who favoured the following explanation: residual (unextractable) dye molecules remaining in the silica gel act as attraction centres for specific adsorption, and are the main species responsible for the specific adsorption of matching dye species.[21] In other words, their findings led them to believe that unextractable dye molecules acted as a sort of crystallization centre (holding only loosely to the definition) onto which other molecules would stick, and to reject the idea that silica gels acted as specific adsorbents as a result of lock-and-key-type interactions between targets and physical cavities in the matrix. Their theory was based in part on their observation that the materials they made showed constant leaching of the imprint, indicating that a significant amount of the imprint molecule remained in the gel after the extraction step.

Perhaps one of the most significant arguments that Morrison and coworkers could make against the mechanism Dickey had first proposed was that silica as a matrix is extremely complicated, and prone to such problematic behaviour as reactivity at incompletely condensed moieties and therefore shrinkage upon drying. They postulated that any cavities left behind by an imprint molecule must certainly close as the gel dries, and that only unextractable molecules remaining in the silica gel could preserve the cavities they created. Research into this debate did not succeed in disproving the idea of attraction centres, and although it pointed most strongly to a true imprinting mechanism, the issue remained unresolved.

Research in molecular imprinting shifted away from silica in the 1970s, after to the first two reports of molecular imprinting in organic polymers appeared in 1972: Wulff used an imprint molecule that was covalently bound to the polymer matrix;[22] Klotz added methyl orange dye to a polymerization mixture in a noncovalent manner similar to earlier imprinting in silica.[23] The wide range of organic polymer precursors and compatible functional monomers available, coupled with the limited number of silica precursors available at the time, is the likely reason that molecular imprinting in silica declined so sharply. Additionally, early researchers in molecular imprinting were organic and biological chemists, so it is not surprising that they chose to work with organic polymers rather than with inorganic substances like silica. Indeed, the dominant context for molecular imprinting in the 1970s and 1980s was focused on biomimetic concepts like enzyme mimics, biological receptors, and artificial antibodies.[24,25]

With the transition to organic polymers for molecular imprinting came a wider variety of methods to create imprint sites, as more easily manipulated molecular precursors and solvent systems offered a full range of covalent and noncovalent interactions. These methods have been studied extensively over the last four decades, and although the range of specific methods is as broad as the selection of molecular precursors available, they can be grouped into categories based on the dominant interaction(s) between the imprint molecule and the functional monomer.

Types of molecular imprinting

Molecular imprinting is achieved by a combination of covalent and non-covalent interactions between a chosen imprint molecule and complementary functional monomers, the exact constellation of which distinguishes the different types of molecular imprinting from each other (Fig. 4). In the first step, an imprint–functional monomer complex (IC) is assembled *via* the appropriate interactions, depending on the method of imprinting chosen. A compatible cross-linking monomer is then used to form the solid MIP matrix. Depending on the imprinting method, the complex formation occurs either before crosslinker addition or *in situ* during polymerization of the matrix. Removal of the imprint molecule through disruption of the functional monomer–imprint interactions liberates an imprint cavity of a defined size and shape. This cavity has the residual organic functional groups of the functional monomer(s) bound in a precise configuration to the inner surface, which can then preferentially interact with a target molecule of an appropriate size, shape, and chemical structure.

Here, we present only conceptual overview of the key characteristics of each type of molecular imprinting. A more thorough discussion with numerous examples of each type of imprinting

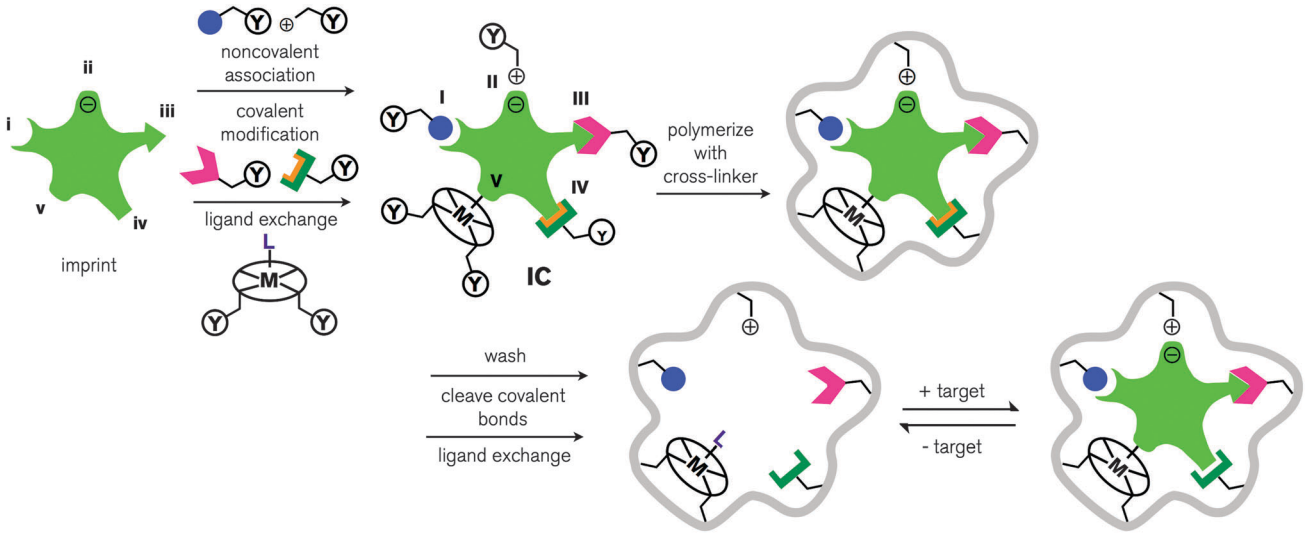

Fig. 4 Five main types of molecular imprinting: (i) noncovalent, (ii) electrostatic/ionic, (iii) covalent, (iv) semicovalent, and (v) metal centre coordination. An imprint molecule is combined with an appropriately chosen functional monomer, through noncovalent, covalent, or ligand (L) to metal (M) interactions with complementary functional groups on the imprint. A complex of the imprint and functional monomer (IC) is formed, in which the functional monomer is bound to the imprint molecule (I) by hydrogen bonding or van der Waals interactions, (II) by electrostatic or ionic interactions (the charges on the imprint and functional monomer may be reversed), (III) through a covalent bond, (IV) through a covalent bond with a spacer (orange), or (V) by ligand–metal or metal–ligand coordination. The functional monomer contains a functional group, Y, which is able to undergo a cross-linking reaction with an appropriate cross-linker. After polymerization of the complex with a cross-linker to form the solid polymer matrix (grey), the imprint–functional monomer interactions are intact. The imprint is removed through washing, cleavage of chemical bonds, or ligand exchange, and leaves behind an imprint cavity with functional groups on the walls. Subsequent uptake of a target molecule is achieved by noncovalent interactions (in types i, ii and iv), the formation of a covalent bond (in type iii), or by ligand exchange (in type v) with target molecules that fit into the cavity and possess the correct structure. The matrix may also participate in target recognition and binding through non-specific surface interactions that results from surface features created around the imprint molecule during cross-linking. Adapted from ref. 9.

can be found in an excellent review.[9] The discussion presented here covers some of the general features of each type of imprinting, but the particulars may vary depending on the system selected.

Noncovalent imprinting. Noncovalent molecular imprinting can proceed by ionic or nonionic interactions. Most commonly, the dominant interaction is hydrogen bonding, which occurs for example between methacrylic acid groups and primary amines in nonpolar solvents.[26] The main advantage of this method is the absence of bond-formation-related kinetic barriers to IC formation and target molecule recognition; instead, the dominant limiting factor is diffusion, which can be easy to mitigate with carefully chosen system parameters. However, such weak interactions require the use of an excess of functional monomer because the equilibrium of the system does not favour the formation of the IC. Ionic interactions such as the formation of ion pairs are dominant in polar solvents and are strong enough to allow for the formation of stoichiometric ICs.[27] This reduces the occurrence of non-specific binding sites in the final MIP.

Noncovalent imprinting is certainly a simple method, particularly when ICs self-assemble in the pre-polymerization mixture. However, noncovalent imprinting is sensitive to even slight disruption of the interactions holding the complex together (for example, the presence of water), and is therefore not very robust. Additionally, if excess functional monomer is present, the existence of nonspecific binding sites where excess functional monomers were incorporated into the matrix can affect the selectivity of the MIP. While it is possible to cap these excess groups in a post-polymerization step,[28] this treatment must be done with the utmost caution and control, as it can easily disrupt the desired interactions and damage imprint cavities.

Covalent imprinting. In order to achieve highly specific imprinting and target binding that is robust, the use of reversible covalent bonds is an obvious choice. This is one of the classical methods of molecular imprinting,[24] and often uses such readily reversible condensation reactions as those that form boronate esters,[29] ketals/acetals,[30] and Schiff's base.[31] Covalent imprinting, being stoichiometric, ensures that functional monomer residues exist only in the imprint cavities; this can greatly reduce nonspecific interactions. However, the need for a distinct synthesis step to generate the initial IC, as well as the bond cleavage required to remove the imprint and bond formation required to bind a target molecule increase the complexity of this method, and the additional kinetic barrier of covalent bond formation may render it slower in target binding. Additionally, only a limited number of functional groups may be imprinted using the covalent method, which results in this approach being less versatile overall.[9]

Semicovalent imprinting. An optimized combination of the durability of covalent imprinting and the rapid target uptake of noncovalent imprinting (where the dominant kinetic barrier is diffusion of target species into the imprint sites), semicovalent imprinting most commonly makes use of a small sacrificial spacer fragment, such as carbon dioxide.[32] This spacer adds just enough length to the covalent bond holding the IC together

to facilitate the transition from covalent bonds in the imprinting step to noncovalent interactions in the target uptake step. Despite the additional step required to synthesize the initial, covalently attached IC, the final target uptake step proceeds by rapid noncovalent binding. This method combines the precision of covalent imprinting in the creation of the imprint cavity with the speed of target uptake characteristic of noncovalent imprinting.

Imprinting using coordination chemistry. Metal ions can participate in imprinting in one of two ways: either they form part of a complex that is covalently bound to an imprint cavity and participate in target recognition through metal–ligand bonding interactions (where the target is a ligand for the metal ion in question, Fig. 4v), or they can act as the actual imprint when metal ion uptake is the goal. When a metal ion is the centre of a complex that is bound to the walls of an imprint cavity, it can undergo ligand exchange to bind an appropriate target molecule. The range of choices for the metal and its ligands is vast, making this method easy to tailor to specific needs, providing at least one of the most strongly bound ligands contains a polymerizable moiety that is compatible with an appropriate crosslinker. Another key criterion is that the ligand exchange between the placeholder ligand (L, Fig. 4) and the imprint molecule (and later the target) occurs under conditions compatible with the system in question.[33] Alternatively, a metal ion may act as an ionic imprint species to create an imprint cavity that can interact with an appropriate target metal ion (not shown in Fig. 4). In this case, the ligands that are covalently bound to the matrix persist, and the metal ion is removed after imprinting. The level of selectivity that is possible in this kind of imprinting is governed less by the size of the cavity created (in other words, it is less likely that the size-selectivity that exists in the imprinting of relatively complex organic molecules exists here) and more by the (partial) charge that exists in the cavity and the strength of the interactions between the target metal ion and the ligands in the cavity.[34]

Combining methods and optimization. Although each of the previously discussed methods of molecular imprinting may be used on its own, combinations of the different types are also useful. For example, a combination of ionic and hydrogen bond interactions can enhance the overall effectiveness of a noncovalent imprinting system.[35] The choice of combination depends on the imprint and target, the matrix, the synthesis conditions, and the intended application of the MIP.

The types of molecular imprinting are categorized according to the functional monomer–imprint interaction present. However, the choice of cross-linker, polymerization method, porogenic additive, and solvent(s) will also influence the performance of the MIP. Exploiting non-specific binding interactions between target molecules and the crosslink matrix, for example, can serve to enhance the target retention. Conversely, these interactions can have detrimental consequences on a system's selectivity. MIP optimization needs to take into account a wide variety of factors that extend far beyond the type of imprinting selected.

Interactions in molecular imprinting. So far, we have looked at the specific interactions that occur between complementary functional groups on imprint molecules and functional monomers. Depending on the imprinting strategy selected, the binding energies of noncovalent interactions in the system may vary (Table 1).[36] If a covalent imprinting strategy is used, the binding energies will be significantly higher, but if a semicovalent approach is used, the noncovalent interactions that also participate in the formation of imprint sites will not be negligible during target binding events. When considering an imprinting strategy and selecting an imprint molecule, it is useful to consider the following general concepts:[36]

Table 1 Summary of binding energies of noncovalent interactions

Type of binding interaction		Binding energy (kcal mol^{-1})
Electrostatic	Ion–ion	20–80
	Ion–dipole	12–50
	Dipole–dipole	1–10
Coordination bonding		20–50
Hydrogen bonding		1–30
π–π stacking		0–12
van der Waals interactions		0–1.5

(1) There must be at least one binding interaction possible.
  (a) The choice of imprint and functional monomer should ensure complementarity.
  (b) Additional interactions may also exist.
(2) Stronger binding interaction(s) are better.
  (a) Covalent imprinting affords a narrower distribution of binding sites, but results in slow or energetically costly target binding events.
  (b) There should be a balance between the strength of IC-forming and target binding interactions before and after MIP polymerization.
(3) More selective binding sites are produced from interactions with specific directionality.
  (a) Species that can bond in more than one direction (such as primary amines participating in hydrogen bonding) afford lower selectivity.
(4) Better binding and selectivity arise when more interactions between the imprint and the polymer are present.
  (a) Nonspecific interactions between the crosslinker and the imprint can enhance binding and selectivity.
  (b) Rigid species reduce the conformational freedom within an imprint site and improve selectivity.
(5) In a bi- or multifunctional imprint, selectivity by interactions with multiple functional groups is best when the intramolecular separation of the groups is maximized.
  (a) Greater spacing between functional groups results in reduced interference.

While these statements are not always true, and a balance must be struck when optimizing different parameters of an imprinting system, they do serve as useful guidelines to consider when designing a new molecular imprinting strategy. It is clear that the choice of imprinting method and molecular precursors requires some thought, and that a strategic approach with the intended application(s) kept in mind is best.

Evaluating imprinted polymers

The evaluation of a MIP generally involves the use of a range of target molecules: the imprint molecule itself, any number of structurally similar species, and other molecules that are significantly different from the imprint in size, structure, and/or shape. In a static binding test, the most common method of evaluation, a known mass of MIP is added to a solution of known target concentration. The system is allowed to come to equilibrium, and the change in concentration of target in the solution is found. This allows the amount of bound target to be determined by difference.[36]

It is customary for initial target binding experiments in imprinted polymers to be conducted in the same solvent used in the synthesis of the polymer.[9] This is mainly due to the variety of interactions that take part in the imprinting process, and the sensitivity of many of them to environmental factors like the polarity, acidity/basicity, and ion content of the solvent, which either enhance binding or compete with it.[37] Because organic polymers are, for the most part, synthesized using organic solvents, this can severely limit their application for biological and environmental samples, with are commonly or sometimes necessarily prepared in aqueous media. If a different solvent is used, it is not guaranteed that the binding interactions will be the same as in the imprinting.

Batch rebinding. In batch rebinding, precise masses of MIP are suspended in solutions containing precisely known concentration(s) of target molecule(s).[38] Targets other than the imprint molecule include structural analogues, larger targets to prove size exclusion in the imprint cavities, and similar targets that lack the required functional groups for specific binding. Batch rebinding experiments are typically fitted with classical adsorption models. The binding event for a target T in solution exposed to a sample of MIP of known mass and allowed to reach equilibrium is described by

$$\mathrm{MIP} + \mathrm{T} = \mathrm{MIP{:}T} \quad (1)$$

and the partition coefficient K_p is

$$K_p = [\mathrm{MIP{:}T}]/[\mathrm{T}] \quad (2)$$

which is found by measuring the difference in target concentration in solution after the binding event. This is an equilibrium constant, and can be used to calculate the free energy of binding:

$$\Delta G = -RT \ln K_p \quad (3)$$

From the difference of the free energies of binding of two targets, we find that to evaluate the selectivity of the MIP for target T_1 over T_2 with a different structure, the ratio of their partition coefficients gives the selectivity factor, α:

$$\alpha = K_{p1}/K_{p2} \quad (4)$$

To determine if a true imprint feature has been created, the imprinting factor IF is found by comparing the MIP and its corresponding NIP for a given target:

$$\mathrm{IF} = K_{\mathrm{MIP}}/K_{\mathrm{NIP}} \quad (5)$$

A value greater than one confirms an imprinting effect, and the greater the value of IF, the more pronounced the imprinting effect.

The time required to reach equilibrium can be determined by a kinetic binding study. This follows the same method as batch rebinding, except that aliquots of the suspension are taken at regular time intervals, separated from the MIP immediately, and analyzed to determine the residual target concentration. When the target concentration stops decreasing, the system is considered to be at equilibrium.

Chromatographic separations. Molecularly imprinted polymers can also be used as chromatographic stationary phases, in which case their performance is evaluated by their ability to resolve mixtures of targets. A very thorough discussion of the different kinds of chromatographic separation methods used with MIPs can be found in the review literature.[9] A MIP powder with a sufficiently narrow particle size distribution may be packed into a standard HPLC column. Alternatively, solid-phase extraction (SPE) is a common method used to test imprinted polymers intended for preparative or separation applications. The general method involves three steps: loading the cartridge with a mixture of species in solution, rinsing the cartridge with a solvent to remove weakly bound species, and finally eluting the cartridge with a strong solvent to collect strongly bound species. Provided the SPE process is performed under equilibrium conditions, the relationships presented in the discussion of batch rebinding may also be used to evaluate the MIP.

An important note to keep in mind is that MIPs contain a distribution of binding sites, which are of varying quality in the binding event. Because there is a distribution, and because the interactions that are present in the binding event are sensitive to experimental conditions (solvent, pH, ionic strength, temperature, competing species), it is important to ensure that comparisons are made primarily for values obtained under the same experimental conditions. If experimental conditions are different, it is essential to note this when making comparisons.

Final note on performance of MIPs. The early work in molecular imprinting was inspired by a desire to mimic the recognition processes that occur in biological systems, particularly enzyme–substrate and antibody–antigen binding events. Compared to biological systems, however, MIPs are inferior. Unlike enzymes and antibodies, which contain perfectly formed and selective homogeneous binding sites, MIPs almost invariably contain a heterogeneous distribution of strong and weak binding sites. The strength of binding in antibody–antigen (Ab–Ag) systems is quantified in terms of the dissociation constant, K_d:

$$K_d = [\mathrm{Ab}][\mathrm{Ag}]/[\mathrm{AbAg}] \quad (6)$$

which, in a heterogeneous phase system like a suspension of MIP in a solvent, is simply the reciprocal of the partition coefficient in eqn (2), and a lower value of K_d corresponds to better overall binding. In biological systems, the values of K_d are generally on the order of between 10^{-9} and 10^{-15} M.[39] By contrast, MIP materials have K_d values on the order of 10^{-3} to 10^{-6} M.[9] In general, while MIP materials have been shown to perform very well for chromatographic separation applications and as sensors when sensitive reporter species are used to signal a binding event, MIPs are still inferior to nature in such biological applications as biosensing and biocatalysis.

Sol–gel silica from molecular precursors

As previously stated, a likely reason for the decline in the use of silica for molecular imprinting was the limited number of silica precursors available in the 1970s compared to the wealth of molecular precursors available for organic polymers. However, the rise of sol–gel methods in the 1980s created a new avenue by which to achieve molecular imprinting in silica.[40] In particular, the work of Schmidt in the mid-1980s on "developing composites on an atomic scale" that could combine the chemical properties of both organic and inorganic materials was an important step for modern work in hybrid organic–inorganic materials.[41,42]

The sol–gel method

Sol–gel methods use metal alkoxide molecular precursors to produce a metal oxide according to the overall reaction

$$n\mathrm{Si(OR)_4} + 2n\mathrm{H_2O} \rightarrow n\mathrm{SiO_2} + 4n\mathrm{ROH}$$

where R is an alkyl group and the metal in this case is Si.[43] The precursors first form a colloidal solution (a sol), then an integrated network (or gel) of amorphous material. For silica, tetraalkoxysilanes (such as tetramethoxysilane, TMOS, or tetraethoxysilane, TEOS) hydrolyze and polycondense to form highly cross-linked silica materials.

The reactions proceed either by acid catalysis at pH < 2 or by base catalysis at pH > 2 (Fig. 5). The crossover at pH = 2 marks the isoelectric point of silica, where the electric mobility of silica is zero and reaction rates are extremely low. Sol–gel processing is done at low temperatures (generally between 0 °C and 100 °C) and in mild chemical conditions (pH and water content are easily tunable). Although the balanced reaction suggests that two equivalents of water are sufficient to produce one equivalent of completely condensed SiO_2, this is rarely the case. Depending on the porosity of the final material, a significant amount of incompletely condensed SiOH and sometimes SiOR species will be present. The precise amount can be determined by techniques like solid-state ^{29}Si NMR, and the true empirical formula for sol–gel silica is written as $[SiO_x(OH)_y(OR)_z]_n$ where $2x + y + z = 4$. The degree of condensation can be controlled to a certain point by the synthesis method used and post-synthetic treatments to drive off water and alcohol and increase condensation, but this is not necessarily required. The water and alcohol produced in the sol–gel reactions serve as porogens in the material, and when drying is done in ambient conditions, the resultant material is called a xerogel. If drying is done in supercritical conditions, an aerogel is produced. Aerogels have extremely low densities, high surface areas, and large porosities, and they have excellent thermal and electrical insulation properties. However, their extremely large surface area also makes them less robust than xerogels, which have smaller porosities and lower surface areas.

The rate of reaction for hydrolysis depends on pH, water content of the synthesis solution, and the nature of the alkyl group. Generally, larger and/or bulkier alkyl groups slow the rate of hydrolysis. Likewise, steric effects from larger alkyl groups on neighbouring species hinder condensation.

Why imprint in sol–gel silica?

The reasons to use sol–gel silica for molecular imprinting are numerous.[5] Its reactivity is low in all but extreme conditions, which include exposure to very strong acid, very strong base, oxidizers, and toxic fluoride species. This makes it a robust matrix for a wide variety of applications and chemical environments. The rigid, highly cross-linked structure of xerogel silica allows the creation of delicate imprint sites with the potential for a high degree of shape selectivity compared to more flexible organic polymers. This template fidelity is likely a major contribution factor to the success of early silica imprinting work. At the sol stage, tremendous control over the shape of the silica is possible, which will be discussed throughout the case studies presented in the following sections. Silica exhibits minimal swelling in the presence of solvents and shows excellent thermal stability. These attributes, too, allow it to maintain the shape and size of imprint cavities. Silica is very stable against oxidation and ageing, which are problematic in many organic polymers. Silica is also remarkably compatible with aqueous and biological systems, and is able to successfully encapsulate enzymes and antibodies without damaging their activity.[40,44,45]

However, there are also challenges associated with silica's rigid and highly cross-linked structure. Although sol–gel silica is often highly porous, the porosity is disordered and diffusion

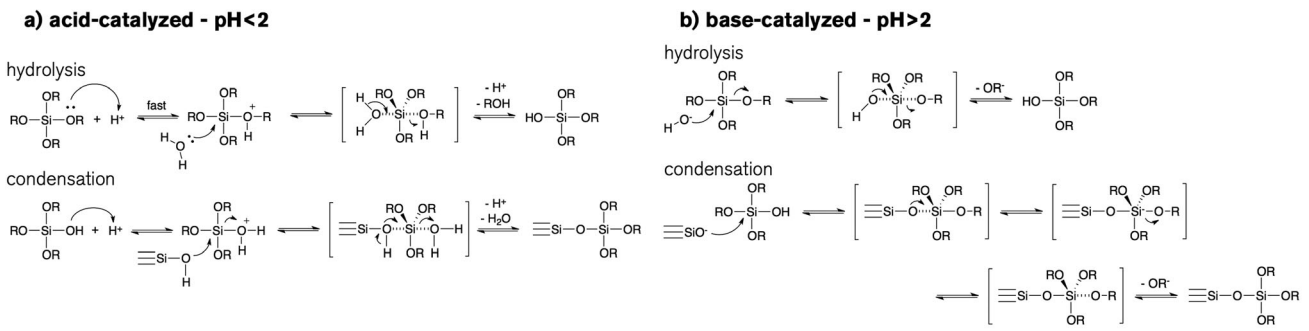

Fig. 5 General mechanisms of hydrolysis and condensation of alkoxysilane precursors to form silica in (a) acid catalyzed conditions and (b) base catalyzed conditions. Condensation can produce either water or alcohol as a byproduct.

pathways are not direct. Because the distance between crosslinks in silica is much less than in organic polymers, silica does not swell easily (in fact, swelling in silica is almost negligible in most cases). Overall, this means that it is crucial to exert control over the diffusion distances and pathways in a silica MIP. This can be done by any combination of incorporating various kinds of porosity, controlling the shape of particles, and shrinking dimensions.

Sol–gel organosilica materials

Atomic-scale composite materials, or hybrid materials, are easily produced by the sol–gel method simply by the addition of molecular precursors that are able to undergo the same hydrolysis and condensation reactions as the metal alkoxide. In silica, these materials are referred to as organosilicas. Organosilica describes any siliceous material in which silicon atoms (some or all) are covalently bound to at least one carbon atom; this can include both materials that have been *modified* to contain organic groups and that were *synthesized with* organic groups. It is common for materials composed of mostly silica (with only a small fraction of Si atoms bound to C atoms) to simply be referred to as silica. However, for the sake of clarity, silica will only be used here to refer to materials that contain no Si–C bonds whatsoever.

Looking at the molecular precursors that are commercially available (Fig. 6), it is easy to see the connection between sol–gel methods and molecular imprinting. The R′ fragment of alkylalkoxysilane groups of the form $(RO)_mSiR'_{4-m}$[46] interacts covalently or noncovalently with an imprint molecule, and the alkoxysilane fragment behaves like the cross-linking group Y (Fig. 4). This allows the easy covalent incorporation of functional monomers into an inorganic silica matrix (Fig. 6a). Crosslinking tetraalkoxysilane monomers of the form $Si(OR)_4$ or silsesquioxane precursors of the form $(RO)_3SiR'Si(OR)_3$ condense with the functional monomers to form the matrix (Fig. 6b).

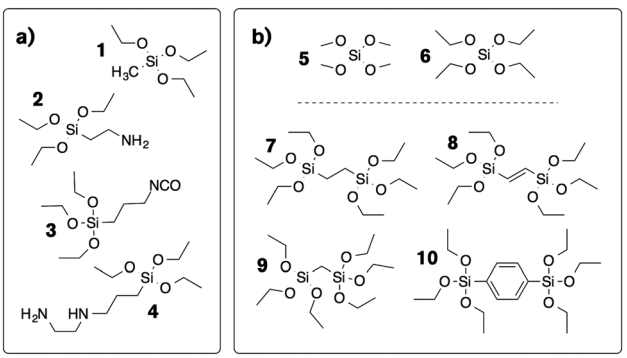

Fig. 6 Structures of selected commercially availably molecular precursors for silica. (a) functional monomers: **1** methyltriethoxysilane (MTES); **2** 3-aminopropyltriethoxysilane (APTES); **3** 3-isocyanato-propyltriethoxysilane (ICPTES); **4** *N*-(aminoethyl)-3-aminopropyl-triethoxysilane (AATES); (b) crosslinkers: **5** tetramethoxysilane (TMOS); **6** tetraethoxysilane (TEOS); **7** 1,2-bis(triethoxysilyl)ethane (BTEA); **8** 1,2-bis(triethoxysilyl)ethene (BTEE); **9** bis(triethoxysilyl)methane (BTEM); **10** 1,4-bis(triethoxysilyl)benzene (BTEB). Ethoxy groups are shown for all structures except TMOS, but many are also available with methoxy groups, which are more reactive.

In contrast to early approaches to molecular imprinting, which simply relied on the formation of cavities in the silica around imprint molecules, sol–gel processing allows organic residues to be covalently bound by Si–C bonds to imprint cavities in the same way they are by C–C bonds in organic MIPs, and participate in the same kinds of target interactions as in all-organic systems. The choice of functional monomer will depend on the imprint molecule, while the choice of crosslinker will depend on the desired properties of the matrix.

Molecularly imprinted organosilica

In the following two sections, representative selections from the literature over the past fifteen years will illustrate the different approaches to preparing molecularly imprinted organosilica (MIO) of different shapes. The work presented here is only a fraction of the literature; many other excellent reports exist that are only omitted here because of a lack of space. The examples are arranged in terms of the morphological control exerted over the matrix, and are divided into two categories according to the smallest length scale at which morphological control is exerted: micrometres and nanometres. The approaches range from simple post-synthetic procedures (grinding and sieving bulk monoliths of gel, spin coating thin films) to highly specific synthetic methods (highly ordered porous materials prepared by micelle templating).

Case studies in micron-scale morphology control

Sol–gel silica is that prepared with minimal additional water or solvent (only enough to effect hydrolysis or prevent phase separation at critical stages) and allowed to gelate and harden as a xerogel monolith takes on shape of its container. Any chemical species (solvent, additives, *etc.*) that are present in solution can become trapped in the matrix, creating pores. Depending on the degree of drying and condensation and the dimensions of the monolith, diffusion can be highly problematic. The customary solution is simply to grind the monolith and sieve the resultant particles to achieve a moderately narrow size distribution in the range of tens of microns.[47]

Imprinting in bulk organosilica monoliths

The Davis group reported the preparation of bulk microporous MIO that displayed a measurable increase in microporosity upon removal of the imprint molecule.[48] Using a semi-covalent imprinting method, the authors prepared imprinted materials using one-, two-, and three-point imprint molecules linked to APTES by a carbamate bond (Fig. 7a). As-synthesized monoliths were ground to a powder of particles smaller than 10 μm before further steps were performed. The powder was treated with chlorotrimethylsilane and hexamethyldisilazane, which reacted with residual silanols in the rest of the matrix to cap them with trimethylsilyl groups. This silanol capping was done in order to avoid non-specific binding interactions between a target molecule and the imprint cavity/surrounding silica matrix.

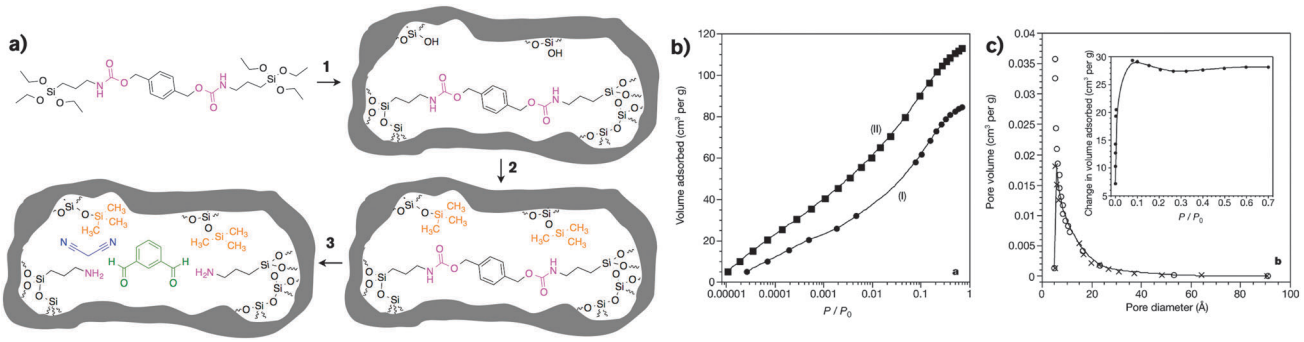

Fig. 7 (a) Imprinting and imprint removal scheme for two-point imprinted material: **1** material synthesis from an IC linked by a carbamate bond (magenta) using TEOS as a crosslinker, water, and HCl as a catalyst, followed by silanol capping with TMS (orange) using chlorotrimethylsilane and hexamethyldisilazane; **2** imprint removal by treatment with trimethylsilyliodide in acetonitrile (0.25 M) and then washing with methanol/aqueous sodium bicarbonate. The imprint cavity is a size-selective base catalyst for the one-to-one condensation of malononitrile (blue) and isophthalaldehyde (green). (b) Argon adsorption isotherm at 77 K on the as-synthesized two-point material (I) and the two-point material after imprint removal (II). (c) Pore size distribution for (I) (crosses) and (II) (circles); inset, difference in volume adsorbed between (II) and (I). Reproduced with permission from ref. 48. Copyright 2000 Nature Publishing Group.

Cleavage of the carbamate bond to remove the imprint was achieved using trimethylsilyliodide. Gas adsorption before and after imprint removal showed an increase in overall volume adsorbed (Fig. 7b), which corresponded to the introduction of additional microporosity (pore diameters smaller than 20 Å) through the post-synthetic treatment steps (Fig. 7c). The authors attributed this added porosity to the imprint cavities vacated after imprint removal. As can be seen in the pore size distribution, all of the porosity is in the micropore range, which corresponds to very narrow diffusion pathways for solvent and target molecules to travel. The two-point imprinted material was used as a base catalyst for the Knoevenagel condensation reaction between malononitrile and isopthlalaldehyde, which was restricted to a one-to-one ratio in the imprinted material because of the size restriction inside the imprint cavities. A control amorphous silica with surface aminopropyl groups was able to condense a second malononitrile molecule to the second aldehyde, which the authors used to confirm the size-selectivity of the imprint cavities.

In this report, no direct discussion was given of the need for small particles. It is reasonable to assume that previous literature in which imprinted bulk monoliths were ground to a powder informed the decision. Although no direct experimental evidence of improved diffusion as a result of the grinding was presented, the catalytic turnover rate of 74 per amine site per hour, as compared to 367 turnovers per hour for surface amine groups in the control material indicates that moderately good diffusion rates were achieved in the particles. However, the fact that the catalysis in the MIO proceeded at only one-fifth the rate of the control clearly shows the influence of access on the performance of the material. This report was one of the early successes in the revitalization of molecular imprinting in silica, and continues to appear as a reference in more recent work. The carbamate bond used in this example is a popular linker for MIO materials because it is easy to form and cleave[49] and is stable for most of the chemical environments used in sol–gel processing. The sacrificial spacer, CO_2, widens the overall imprint site slightly, and facilitates non-covalent interactions like hydrogen bonding.

Imprinted silica/organosilica spheres

Although it is a simple procedure, mechanical grinding to produce a powder from a monolith has the distinct disadvantage of poor material economy: the effort to obtain at least a moderate particle size distribution can result in the loss of up to 80% of the total material.[50] This loss is unacceptable for any sort of industrial or commercial application. One alternative to mechanical grinding is to vary the synthesis conditions and produce particles directly. The Stöber method from 1968 is a well-established protocol for producing silica spheres in solution from the ammonia-catalyzed reaction of tetraalkyoxysilanes in alcohol.[51] After more than 40 years of development, variations of this method abound, and include the use of different solvents, catalysts, and additives. Depending on the intended application, the degree of polydispersity in size is easily tuned. Excellent size control from tens of nanometres up to several microns has been demonstrated through synthetic and templating approaches.[52,53] The typical process involves creating small monodisperse seed spheres, and then growing them either continuously or in a stepwise fashion.

The Chang group reported the preparation of spherical MIO particles imprinted for estrone, a naturally occurring estrogen.[54] An estrone IC, formed *via* a carbamate linker, was incorporated into spherical particles of controlled size (between 1.5 and 3 μm in diameter) using TEOS as a cross-linker (Fig. 8a). Two final MIO materials were produced by using a different nucleophile in the carbamate cleavage: H_2O (OH^-) produced Imp-A with a terminal amine group, while ethylene glycol ($HOCH_2CH_2O^-$) produced Imp-B with a terminal alcohol. Anticipating the difficulty of removing molecules from the centre of micron-sized particles of highly cross-linked organosilica, the authors controlled the placement of the imprint sites by adding the IC partway through the synthesis of the particles, thus creating core–shell SiO_2@MIO spherical particles (Fig. 8b).

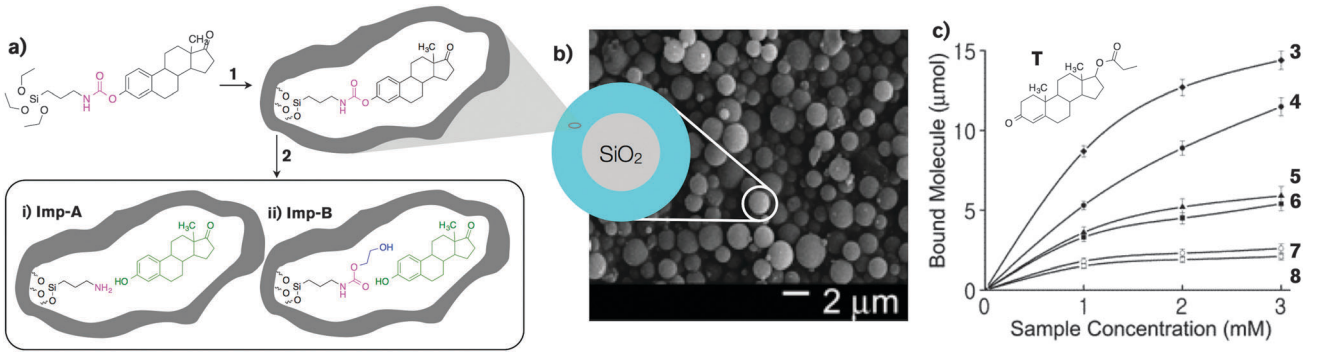

Fig. 8 (a) Imprinting and imprint removal scheme for estrone imprinted core–shell spheres: **1** material synthesis from an IC linked by a carbamate bond (magenta) using TEOS as a crosslinker, *n*-decyl alcohol, hydroxypropyl cellulose, and sorbitan monoorleate as additives, and aqueous NH_4ON as a catalyst; **2** imprint removal by thermal treatment in DMSO with (i) H_2O to produce Imp-A with a terminal amine or (ii) ethylene glycol to produce Imp-B with a terminal alcohol (blue). Target interaction with estrone (green) likely goes by hydrogen bonding. Control silica particles were prepared with APTES instead of the IC and in the absence of estrone. (b) Scanning electron micrograph of spheres produced, showing schematic representation of structure of the particles and the location of the imprint sites (turquoise). (c) Amount of bound estrone by **3** Imp-B, **4** Imp-A, and **5** the control; amount of bound testosterone propionate by **6** Imp-B, **7** Imp-A, and **8** the control. Reproduced with permission from ref. 54. Copyright 2002 American Chemical Society.

Confirmation of the position of the imprints was obtained by changes in FTIR spectra corresponding to loss of imprint functional groups after mechanically grinding away the outer shell. No mention is made of the estimated thickness of the shell (or the depth at which imprint sites would be buried). Static binding tests were performed in chloroform for two targets (estrone and testosterone propionate), and interestingly Imp-B showed the best binding behaviour overall for estrone (Fig. 8c). The authors did not speculate as to the reason the alcohol-terminated imprint cavity showed better binding performance than the one with the amine, but did point out the possibility of introducing a variety of different functional groups (perhaps with reference to groups not compatible with the synthesis of MIOs by the sol–gel method) in a post-synthetic step. This example shows a deliberate attempt to circumvent the diffusion problem that may be encountered in highly cross-linked sol–gel silica. The ease with which additional layers of (organo)silica can be added to existing material through particle regrowth and grafting is a very positive attribute of silica.

Imprinting in thin films

One of the great advantages of sol–gel processing is the ease with which sols can be used to produce thin films of high quality. Most commonly achieved through spin-coating, films of controlled thickness can be prepared on a variety of substrates by adjusting the spinning speed during the coating process and controlling the viscosity of the sol by varying the aging time before coating (viscosity increases over time). The obvious advantage of thin films is the fact that they are thin; shorter diffusion lengths than in bulk sol–gel silica are produced inherently, which means the binding kinetics for imprint sites should be higher. Also, films can be coated on a variety of substrates commonly used in sensor assemblies, making it easy to integrate custom sol–gel materials to build new sensors. However, challenges do arise from the inherently lower porosity of spin-coated sol–gel thin films, which can impede diffusion as compared to bulk sol–gel materials where larger pore volumes are present.[55]

Early in the development of modern molecular imprinting in silica, the Collinson group reported noncovalent imprinting of dopamine (DA, **4**) in a hybrid sol–gel thin film formed on a glassy carbon electrode substrate from a mixture of three sol–gel precursors: TMOS (**1**) as a cross-linker, methyltrimethoxysilane (MTMOS, **2**) to increase hydrophobicity and film stability, and phenyltrimethoxysilane (PTMOS, **3**) as a functional monomer (Fig. 9a).[56] DA was physically entrapped inside the 450 nm-thick film, presumably in close proximity to **3** as a result of an IC formed by favourable hydrophobic and aromatic interactions. Extraction of the DA imprints was achieved in the final film by soaking it in a phosphate buffer solution for 24 hours and confirmed by UV-Vis spectroscopy. A non-imprinted control film was prepared in the same manner but in the absence of DA. To test the film's sensing capabilities, it was exposed to buffered aqueous solutions (pH 7) of various targets and the normalized voltammetric response of the film was recorded (Fig. 9b). Similar responses were observed for **4** and **5**, which is expected for an target with the same key functionality (in this case, the catechol ring) but a smaller size (no 2-aminoethane group). Size selectivity was confirmed by normalized responses for structurally similar molecules of varying chemical functionality at the 4 position on the aromatic ring (**6**, **7**), of larger size (**8**), or of zwitterionic (**9**) or acidic nature (**10**) in aqueous buffer solution. Structures **6** and **7** showed about half the response of DA, while **8**, **9**, and **10** showed no measurable response. The sensor film is likely negatively charged in pH 7 buffer, which can explain the exclusion of negatively charged species that cannot participate in the same interactions as the imprint molecule. Exclusion or poor recognition of larger or bulkier targets than the imprint is often used as evidence for imprint sites that are size-selective.

The response time of the film was evaluated by the time required for stabilization of the peak current; this was achieved in five minutes or less. Based on the lack of voltammetric

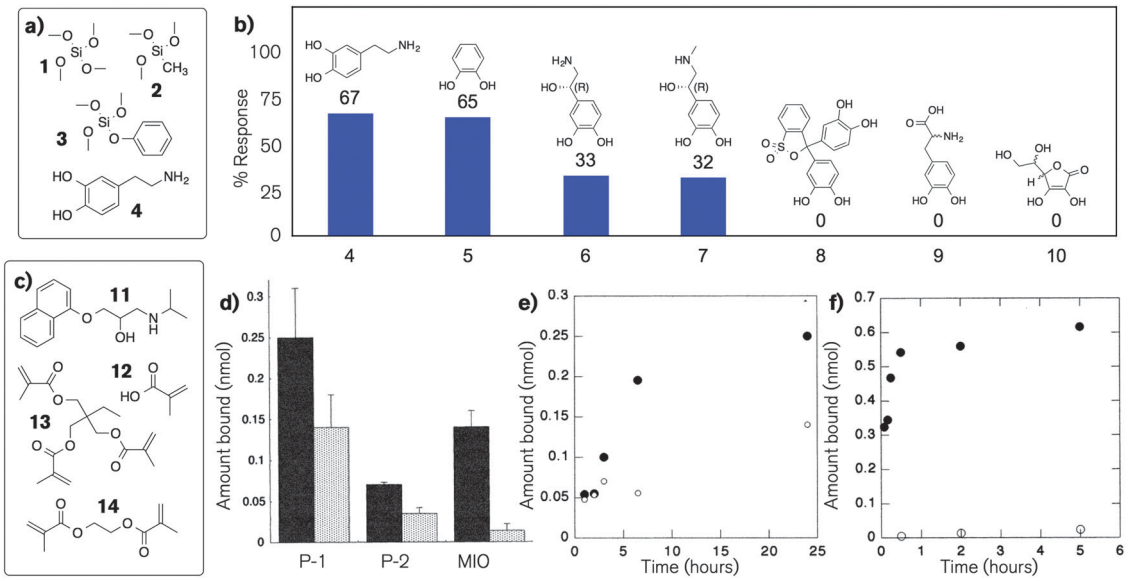

Fig. 9 (a) Sol–gel precursors and imprint molecule for noncovalently imprinted thin film sensor: **1** TMOS; **2** methyltrimethoxysilane (MTMOS); **3** phenyltrimethoxysilane (PTMOS); **4** dopamine (DA). (b) Percent voltammetric response in imprinted thin film sensor of various targets: **4** dopamine; **5** catechol; **6** norepinephrine; **7** epinephrine; **8** catechol violet; **9** (dihydroxyphenyl)alanine; **10** ascorbic acid.[56] Responses were normalized to the response of that target at a bare glassy carbon electrode. (c) Imprint molecule propranolol (**11**), functional monomers methacrylic acid (MAA, **12**, P-1) and trimethylolpropane propane trimethacrylate (TRIM, **13**, P-2), and crosslinker ethylene glycoldimethacrylate (EGDMA, **14**) for the preparation of an imprinted organic thin film. A MIO film was prepared with **1**, **2**, and **3** as crosslinker and combined functional monomers, respectively, using **11** as the imprint. (d) Steady-state binding of **11** in acrylic (P-1 and P-2) and MIO thin films: imprinted (black) and nonimprinted controls (grey). Kinetic binding of **11** in (e) P-1 imprinted (solid circles) and nonimprinted (open circles) and (f) MIO imprinted (solid circles) and nonimprinted (open circles). Figures d, e, and f reproduced with permission from ref. 60. Copyright 2001 American Chemical Society.

response observed for all targets in the non-imprinted control film, the authors suggested that the films were likely fairly dense, and that porosity was mostly generated in the imprinted film as a result of DA removal (which would have vacated imprint cavities). However, they noted that it was not possible to directly characterize the porous nature of the film because of the very small amount of organosilica material present on the substrate. Although they did compare AFM images of their films to previously reported work, this point highlights a major challenge when controlling the morphology of thin films. It is entirely possible that greater porosity of the films could contribute to faster response times and better target uptake, but without conclusive evidence of porosity it is impossible to confirm. Gas sorption is a powerful method of characterizing porous materials,[57] but because it requires that the sample's mass be precisely known and cannot distinguish between adsorption on different surfaces, it cannot work with very thin film samples on substrates. Ellipsometric porosimetry with water vapour has recently been used to characterize the porosity (pore volume and average pore diameter) of thin organosilica films,[58] but this technique may not have been readily available at the time this report was published. Unfortunately, in the absence of direct evidence of the difference in porosity of the imprinted and non-imprinted films in this report, it is neither possible to confirm nor refute that porosity is the major reason for the difference in voltammetric response. The difficulty of controlling and then reliably interrogating the porous structure of sol–gel thin films is a significant challenge.[59] However, this early report was one of the first of its kind, and showed excellent evidence for the potential of using sol–gel thin films for sensing.

Marx and coworkers compared the binding properties in both organic and aqueous media of a thin film MIO to an imprinted acrylic thin film for propranolol (**11**),[60] a beta-blocking drug that is an immensely popular archetypal imprint in organic polymers (Fig. 9c). Thin MIO films (700 nm thick) were simple to produce, but a new polymerization system was required to create thin films of the imprinted acrylic polymer (1 μm thick). As with the previous example, PTMOS (**2**) and MTMOS (**3**) were used as functional monomers and TMOS (**1**) was used as the crosslinker in the MIO film (Fig. 9a). Standard spin coating produced a high quality transparent film. The acrylic polymer film was synthesized *via* modified radical polymerization using methacrylic acid (MAA, **12**, P-1) or trimethylolpropane trimethacrylate (TRIM, **13**, P-2) as the functional monomer and ethylene glycoldimethacrylate (EGDMA, **14**) as the crosslinker. Although this polymer combination is the most popular system for molecular imprinting, preparing a high quality thin film of the acrylic polymer is not a trivial achievement. High degrees (80–100%) of cross-linking can be achieved, but this results in opacity, brittleness, and cracking. The solution was to use a functional monomer/crosslinker ratio that reduces the degree of crosslinking (in this case, to 34%) and establish a precisely controlled polymerization environment inside a closed polymerization cell with controlled pressure and atmosphere.

Aside from the complication in producing a high quality organic polymer thin film, the MIO displayed another advantage over the organic system in target binding studies. As a result of the large amount of functional monomer in P-1 and P-2, the organic films showed both high capacity for **11** and high nonspecific binding (shown by high target uptake in the control non-imprinted films, Fig. 9d). This binding behaviour was similar to literature reports of the same system using bulk imprinted acrylic polymer. By contrast, the MIO film showed lower capacity but much lower nonspecific binding (relative and absolute) in the nonimprinted control. The kinetic binding behaviour of the films also showed the superiority of the MIO film: it reached saturation in less than 1 hour and showed minimal nonspecific binding, while P-1 showed a slower uptake profile, only reached saturation after ~10 hours, and showed nonspecific binding that increased with time. Organic solvents used as porogens in organic polymer syntheses are more volatile than the polar protic solvents (water, alcohol) used in sol–gel processing. As a result, despite their low crosslink density, the acrylic thin films likely had lower overall porosity (most of the solvent evaporated during drying) than the MIO film, which resulted in poorer target binding kinetics.

Even rigid and highly crosslinked organic polymers will contain a significant amount of porosity if appropriate porogenic solvents are used. However, unless compatible nonvolatile solvents are selected, the degree of porosity generated can be lower if the desired morphology is a thin film. By contrast, the ease with which porosity can be tuned in sol–gel thin films (despite their lower porosity relative to bulk monolithic sol–gels) gives them a distinct advantage in imprinted thin film applications.

Comparing monoliths to powders to thin films

One benefit to imprinting in thin films is that it facilitates the production of sensing devices, in which short diffusion distances presumably allow for rapid response times. However, complete characterization of an imprinting strategy in organosilica is difficult to achieve if only a thin film is produced. Challenges in physicochemical characterization for thin films arise because of the very small amount of MIO produced in a single film (*vide supra*); this is an unnecessary evil, given the ease with which gram-scale amounts of silica-based sol–gel materials can be produced at low cost. Therefore, whenever possible, the preparation of various morphologies of the same MIO is useful for obtaining a more complete understanding of the characteristics of the system. Naturally, the different processing conditions can introduce variations in the materials, and these must be considered when drawing conclusions, but given the flexibility of the sol–gel method and the ease of changing one variable at a time, it is possible to account for these inconsistencies.

An imprinting approach using multiple morphologies to achieve comprehensive characterization appears in the work of the Bright group, who used 9,10-anthracenediol as an imprint molecule in bulk organosilica and thin films with TMOS as a crosslinker (Fig. 10a).[61] The bulk monolithic materials and thin films were labeled with a polarity-sensitive probe molecule, 4-chloro-7-nitrobenzo-2-oxa-1,3-diazole (NBD), which was used

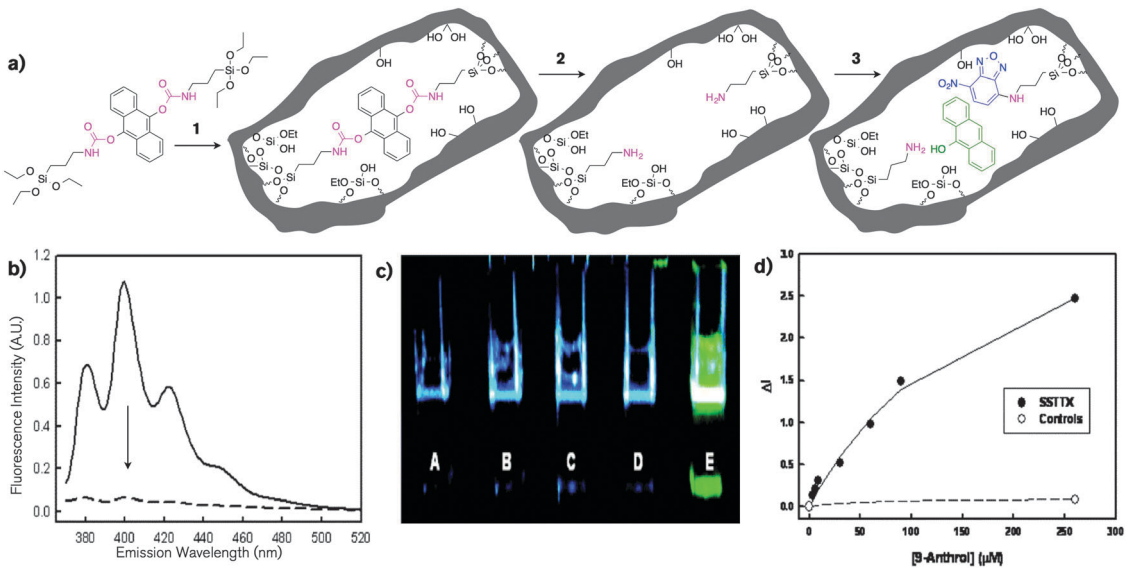

Fig. 10 (a) Imprinting, imprint removal, and site-selective tagging scheme for a site-selective tagged and template xerogel (SSTTX): **1** material synthesis from an IC (BST) linked by a carbamate bond (magenta) using TMOS as a crosslinker, water, and HCl as a catalyst; **2** imprint removal by carbamate cleavage using $LiAlH_4$ in THF under argon; **3** target uptake of 9-anthrol (green) or its tautomer 9-anthrone, followed by site-selective tagging of the second aminopropyl group by the fluorescent probe 4-chloro-7-nitrobenzo-2-oxa-1,3-diazole (NBD, blue) in THF. After tagging, 9-anthrol is washed out to produce a sensor. (b) Steady-state emission spectra from imprinted material in a before (—) and after (- -) $LiAlH_4$ treatment, showing >90% imprint removal. (c) Photograph of monoliths of control materials (A–D) and the SSTTX (E, as prepared in a) excited at 488 nm and filtered for NBD fluorescence only. Controls varied from E as follows: (A) no imprint; (B) noncovalent imprint analogue; (C) one-point imprint analogue; (D) no imprint removal step. (d) NBD response profiles for the SSTTX and controls A–D exposed to varying [9-anthrol]. Controls do not give a significant response, while the SSTTX does. Reproduced with permission from ref. 61. Copyright 2006 American Chemical Society.

to sense the presence of the target by its fluorescence response. After labeling, the so-called site selectively template and tagged xerogel (SSTTX) to detect 9-anthrol, which is structurally similar to the imprint molecule. To achieve a better understanding of the performance of the MIOs, four control materials were prepared to eliminate four possible artifacts, namely fluorescence from nonspecific matrix binding (A), fluorescence from imprint site binding by encapsulation only (B), fluorescence in the absence of the target molecule (C), and fluorescence from NBD not covalently bound in the imprint site or other undesired fluorescence (D). All five materials (controls A–D and the SSTTX) were prepared as monoliths in duplicate and thin films. One monolith of each material was ground to a fine powder (irregular particles 20–500 μm in diameter), and one was left whole. The maximum diffusion length for imprint sites buried most deeply in the material varies from 2 μm for films to as much as 250 μm for particles (assuming a maximum diameter of 500 μm) and 0.5 cm for monoliths (which were prepared in 1.0 cm cuvettes). Longer reaction times were accordingly allowed for longer diffusion distances: the imprint removal step by treatment with $LiAlH_4$ in THF was performed for various times depending on the material morphology: 10–20 minutes for thin films, 24 hours for powders, and at least 48 hours for monoliths. Likewise, washing to remove cleaved imprints, loading of 9-anthrol, and labeling with NBD were carried out for longer times in samples with longer diffusion lengths. Confirmation of successful imprint cleavage and removal was confirmed through the steady-state fluorescence from the anthracene moiety; long reaction and washing times resulted in the removal of more than 90% of the imprint from the monolithic imprinted material (Fig. 10b).

Monolithic samples were used to confirm that the complete SSTTX system was responsible for a positive response to the target by comparing fluorescence signals. Control materials A–D showed no analytical response, whereas the SSTTX (E) showed significant fluorescent response when excited at 488 nm (Fig. 10c). Also of note in this result is the uniformity of the intensity of fluorescence throughout monolith E (not easily seen in the figure). This suggests a uniform distribution of the imprint sites throughout the monolith, which is a highly desirable result if the monolith is to be ground to a powder for separation applications. Obtaining confirmation that the binding sites are homogeneously distributed throughout a MIP is not trivial.

Of note here is the time allowed for the target to penetrate the monolith: it was exposed to a solution of 9-anthrone for fifteen minutes. Conversely, the 2 μm thick film sample exhibited 90% of full scale fluorescent response after 45 seconds of exposure to the target in solution. This is a relatively long response time, which is to be expected for a dense organosilica film. Increasing porosity has been shown to have a significant impact on diffusion of gases in sol–gel thin films[62] and the corresponding response time of thin film sol–gel gas sensors.[63] Accordingly, even in thin films with single micron diffusion lengths, the porosity of the material will affect response times for sensing small molecules that would require even greater pore sizes for easy diffusion than diatomic gas molecules.

The main reason to use different morphologies to characterize the same MIO system is that different shapes give different information. Film thicknesses are remarkably easy to vary, which would allow for the construction a calibration curve of the response time of a sensor as a function of diffusion length, provided porosity is controlled. Monoliths with the fluorescent response in the example above are useful for interrogating the distribution imprint sites. Powders are easily packed into columns for multiple cycles of response testing, repeated separation runs, or easy determination of the response as a function of target concentration (Fig. 9d). Altogether, the different pieces of information that the various MIO morphologies give contribute to a complete understanding of many aspects of the imprinting system.

Case studies in nanoscale morphology control: templated pores

Ideally, MIO materials would be prepared with minimized diffusion through very small dimensions in at least one direction. This is possible to a limited extent by grinding monoliths to very fine powders (three-dimensional decrease in diffusion lengths) or spinning ultra-thin films (one-dimensional decrease), but even these approaches are unlikely to achieve nanometre diffusion lengths. Thin films that are tens of nanometres thick are easy to fabricate, but the resultant decrease in the volume of MIO material translates to fewer imprint cavities, which means that the signal to noise ratio may suffer for sensing applications. Optimization of any one parameter often results in compromises in another.

As previously discussed, thin films are inherently denser than monoliths, and the decrease in diffusion length achieved is likely to be counterbalanced by an accompanying decrease in porosity. Thus, the best solution to the problem of improving diffusion to achieve fast imprint–target interactions in rigid polymers like organosilica is porosity. Studies have clearly shown that porosity affects diffusion, though it is hardly a logical stretch to understand this point. It is only natural, then, to want to introduce more porosity into molecularly imprinted materials. However, random porosity generated by solvents in bulk organosilica is less than ideal, as the diffusion pathways are not guaranteed to be optimal and the connectivity of pores cannot be controlled.

Templated pores with controlled shape and size

The IUPAC classifies pores into three size categories based on their smallest diameter: micropores have diameters smaller than 2 nm, macropores have diameters greater than 50 nm, and mesopores have diameters between 2 and 50 nm.[64] Pores of irregular shape behave according to the smallest diameter they possess. Long channels that are open at one or both ends are classified according to the diameter and not the length of the channel. Typical solvent pores in bulk sol–gel silica range are a mix of micropores and mesopores with broad pore size and shape distributions. In 1992, a report from Kresge and coworkers gave rise to an entirely new class of sol–gel materials: ordered

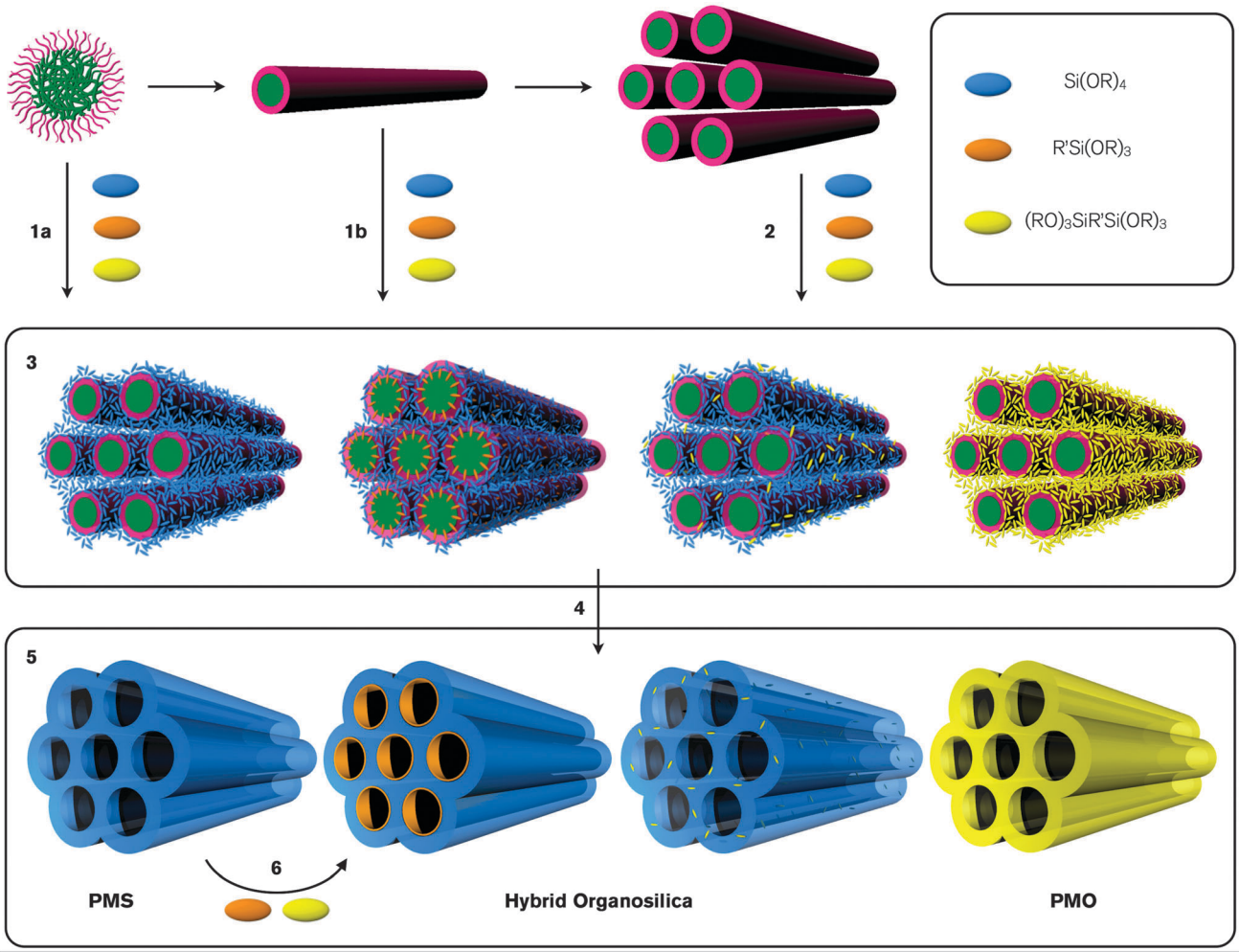

Fig. 11 Schematic representation of the synthetic approach to surfactant-templated mesoporous materials using self-assembly between a template (a typical triblock copolymer shown here) and molecular precursors of different types (blue: tetraalkoxysilane, orange: alkyltrialkoxysilane, yellow: silsesquioxane precursor). The surfactant forms micelles in solution, the shape of which (spherical or rod-like) is determined by concentration. At low template concentrations, cooperative self-assembly (**1a**, **1b**) between micelles and sol–gel precursors occurs to form the liquid crystalline phase. At high template concentrations, a liquid crystalline micelle phase is formed independently, and sol–gel precursors assemble around the micelles when added to solution (**3**). Sol–gel processing through catalyzed hydrolysis and polycondensation followed by removal of the template (**4**) yields ordered mesoporous materials of varying chemical structure (**5**). Periodic mesoporous silica (PMS) is pure sol–gel silica. Hybrid organosilica prepared from cocondensation of a mix of precursor types (either blue + yellow or orange, as shown, or yellow+ different yellow or orange, not shown) will have the R′ group localized on pore surfaces if it is terminal (orange precursor) or distributed throughout the pore walls if it is bridging between two Si atoms (yellow precursor). It can also be prepared by grafting an organosilica precursor onto the pore surface of PMS (**6**). A terminal R′ group will dangle into the pore, while a bridging R′ group will lie on the surface or dangle into the pore, depending on the grafting method used. Periodic mesoporous organosilica (PMO) in this case is pure organosilica where every silicon atom is bound to a bridging R′ group.

mesoporous silica.[65] The addition of a quaternary ammonium surfactant to a sol–gel molecular sieve synthesis produced a highly porous material with an unprecedented structure: the pores were long channels of precisely uniform diameter in the *meso* range, arranged in a two-dimensional hexagonal (honeycomb) lattice. The pore structure of the so-called MCM-41 periodic mesoporous silica (PMS) was templated by the surfactant, which formed a 2D hexagonal liquid crystalline phase in solution.

Intense research activity with different surfactants, sol–gel precursors, and synthetic conditions over the past two decades has led to a massive wealth of ordered mesoporous materials of highly controlled pore size, shape, and arrangement, interesting chemical functionality, and various higher order morphologies tailored to specific applications. Two notable achievements in the first decade were the first successful use of a nonionic block copolymer surfactant template (triblock copolymer Pluronic P123) to produce so-called SBA-15 PMS,[66] which allowed for the synthesis of materials with larger pore diameters (and easier pore size tuning over a wide size range), and the simultaneous first reports of periodic mesoporous organosilica (PMO) materials from three all-organosilica $(RO)_3SiR'Si(OR)_3$-type silsesquioxane molecular precursors: BTEE,[67] BTEA,[68] and 1,2-bis-(trimethoxysilyl)ethene (BTME).[69] In the past decade, ordered mesoporous organosilica has been the subject of many excellent reviews.[70–85]

The basic approach to preparing PMS/PMO involves the organization of molecular sol–gel (organo)silica precursors around a micelle structure of a surfactant or polymer template in solution, acid- or base-catalyzed hydrolysis and polycondensation of the alkoxysilane groups, and removal of the template to liberate a final ordered porous material (Fig. 11). In contrast to molecular imprinting where the desired pores are created by an *imprint*, the desired porosity in PMS/PMO is produced by the surfactant, which in this case is called a *template*. As with bulk sol–gel organosilicas, the variations possible in synthetic approach, chemical composition, and post-synthetic treatment steps allow for a wide variety of mesoporous materials that can be tailored to specific applications. Depending on the synthetic conditions and choice of starting materials, pore diameters in these materials can range from ~3 nm to tens of nanometres. Wall thicknesses are typically between 3 and 8 nm, and particle sizes are easily tuned. PMO materials can be prepared in such controlled morphologies as spheres,[86] hollow spheres,[87] "nanorice",[88] coiled rods,[89] thin films,[90] and freestanding membranes.[91] The materials typically have high surface area, reaching more than 1000 $m^2\ g^{-1}$ in some cases, and allow tunable microporosity in the walls through various processing conditions. The potential for better MIO materials through mesopore templating is quite clear: when open pores are of uniform shape and size, access to porosity is improved,[92] and better imprinted materials are possible.

Interactions in mesopore templating. In order to successfully use a micelle system to template pores in a sol–gel material, there must be at least one type of attractive interaction between the micelle system and the sol–gel precursor(s) at the early stages of hydrolysis and condensation.[74,93,94] Therefore, depending on the template species used, the optimal experimental conditions will involve different interactions (Fig. 12). The template (S, surfactant, or N, nonionic copolymer) can have inherent attractive interactions (a, d, e). Alternatively, mediator ions (M^+, metal cations, or X^-, typically halide anions) enable cooperative self-assembly (b, c, f, g). While surfactant templates form well-defined micelles, the hydrophilic blocks of nonionic copolymer templates can also participate in attractive interactions with the sol–gel species. This can result in the partial or complete penetration of the hydrophilic block into the walls of the templated pores, which can introduce additional microporosity and affect the pore diameter as a result (h, i, j). This penetration can be more pronounced if silsesquioxane precursors with bridging organic groups are used.

Molecular imprinting in PMS/PMO materials faces a particular limitation that is not present in most bulk MIOs: unlike bulk materials (monoliths, thin films) where entrapment of the imprint or IC is certain, the volume of solvent used to synthesize most template mesoporous materials is large enough that the location of the imprint or IC is not certain unless specific control over it is exerted. Noncovalent imprinting of organic compounds is especially challenging, as hydrophobic interactions can overcome IC interactions, and result in the imprint molecule being sequestered within the micelles rather than bound inside the condensing sol–gel phase. Alternatively, a covalently bound IC may interact favourably with a portion of the template, resulting in a material in which the imprint sites are located on the surface of the pores rather than buried in the walls. While this case is not necessarily problematic (as the following section, which deals with imprinting that is deliberately located on pore surfaces, will show), it means that care needs to be taken when making statements about where exactly the imprint sites are located.

Surface imprint grafting on periodic mesoporous silica

One approach to overcoming the diffusion problem that we have not yet discussed is controlling the depth at which imprint

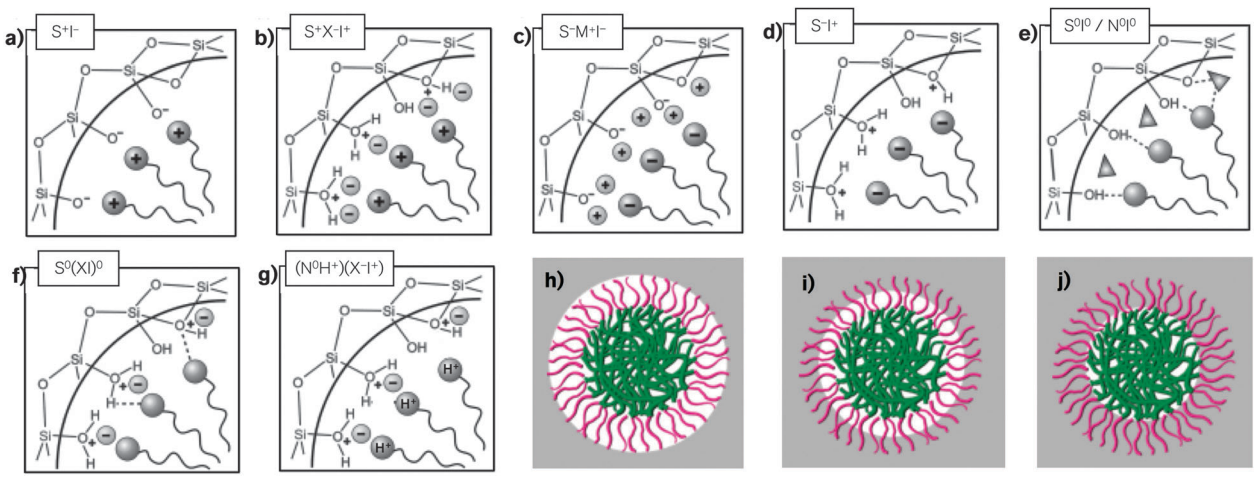

Fig. 12 Interactions between the sol–gel species and the template in acidic, basic, and neutral media.[93,94] Electrostatic interactions are (a) S^+I^- (basic), (b) $S^+X^-I^+$ (acidic), (c) $S^-M^+I^-$ (basic), (d) S^-I^+ (acidic), and hydrogen bonding interactions are (e) S^0I^0/N^0I^0 (neutral) and (f) $S^0(XI)^0$ (acidic). Reproduced with permission from ref. 74. Copyright 2006 Wiley VCH. Additional ionic interactions are possible if a neutral template is protonated in acidic media and a mediator anion is present: (g) $(N^0H^+)(X^-I^+)$. Penetration of the hydrophilic block (magenta) of a nonionic triblock copolymer template into the sol–gel phase (grey) depending on synthetic conditions occurs to varying degrees from (g) not at all to (h) partially to (i) completely, which will affect the templated pore diameter.

sites are located. With the right imprinting strategy, the sites can in fact be located on the surface of a substrate. Grafting alkylalkoxysilanes onto PMS surfaces (as opposed to planar silica substrates) has the distinct advantage of incredibly high available surface area: provided the species to be grafted is size-matched to the pores of the support mesoporous material, hundreds of square metres per gram of surface area are available. This allows for much higher loading of imprints (or any other grafted species) than on planar substrates,[95] while maintaining the fast kinetics of access to surface sites.[96]

Dai and coworkers reported imprint coating in MCM-41-type PMS powder with an average pore diameter of 2.5 nm and a specific surface area exceeding 1000 $m^2\ g^{-1}$. This was achieved by grafting an IC of Cu^{2+} and AATMS (trimethoxysilane analogue of **5**, Fig. 6a) onto the surface of the mesopores (**I**, Fig. 13).[97] A non-imprinted control material was synthesized by grafting pure AATMS with no Cu^{2+} onto another sample of the same PMS (**II**). Additionally, commercially available amorphous silica gel with an average pore diameter of 6.0 nm and a specific surface area of 600 $m^2\ g^{-1}$ was coated with the same IC (**III**). Because amines become protonated below pH = 3 and lose their ability to complex metal cations, removal of the imprint ions was achieved simply by soaking the imprinted material in slightly acidic aqueous solution for 20 minutes and then neutralizing it to pH = 7 before drying. If the uniform shape of pores had no impact on the imprinting effect observed, then similar behaviour should have been observed for **I** and **III** in uptake and selectivity experiments. On the contrary, **I** showed an imprinting factor (IF) for Cu^{2+} of 5.7 over **II** while **III** showed an IF of 1.54. Because the cylindrical pores in the PMS used in this work were of the ideal size for the specific IC used, the authors attributed the better performance of **I** to two major characteristics: pore curvature and size that matched the stereochemical requirements for imprinting the Cu^{2+} ion, and a uniform pore size distribution that limited the coordination environment to the desired configuration. Neither of these characteristics is present in amorphous sol–gel silica, and this report clearly demonstrates the value of mesopores for surface metal ion imprinting. The same group later used cocondensation of the same IC with TEOS to yield a so-called "hierarchically imprinted sorbent material".[98] This phrase highlights the conceptual connection between molecular imprinting and templated mesoporous materials: surfactant templating could arguably be seen as a form of molecular imprinting, but at the supramolecular level. When combined, the methods yield hierarchically porous materials.

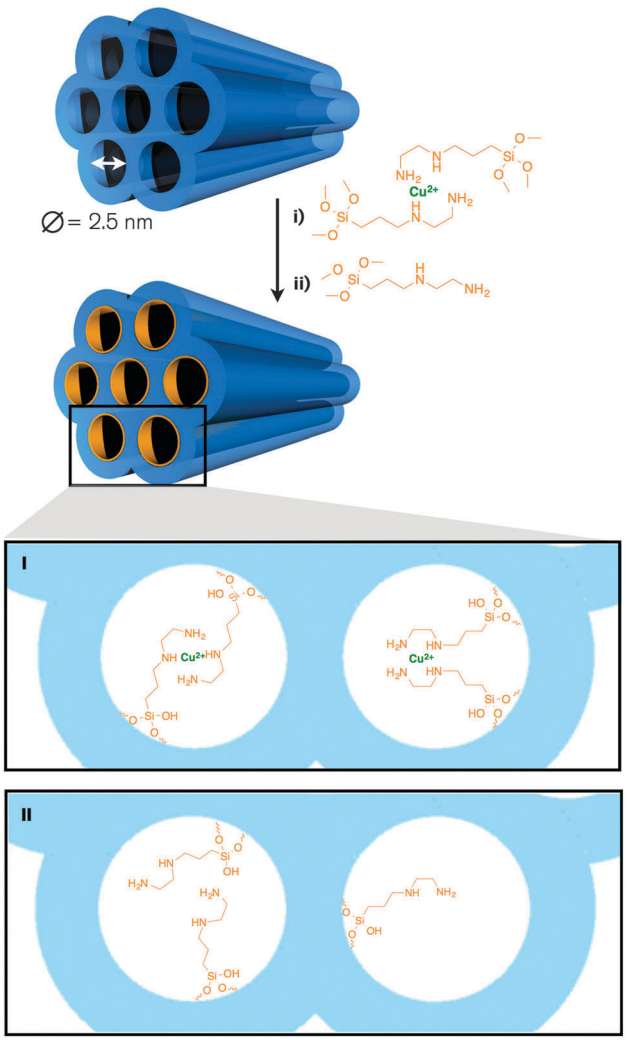

Fig. 13 Schematic representation of imprint coating on MCM-41-type PMS with a pore diameter of 2.5 nm. Grafting of an IC formed between Cu^{2+} and two equivalents of AATMS (i) or pure AATMS (ii) yields a hybrid organosilica material in which the amine moieties are paired and can strongly bind Cu^{2+} (**I**), or are randomly distributed on the surface and not necessarily paired (**II**). Adapted from ref. 97.

Grafted surface imprinting has also been reported in PMS using small molecule imprints. Triangular and rectangular imprint molecules attached by a carbamate bond to APTMS (trimethoxysilane analogue of **3**, Fig. 6a) was grafted onto the pore surfaces of SBA-15-type PMS (Fig. 14a and b).[99] Size-selective imprint cavities in this case were created by capping residual surface silanol groups on the pore walls with octadecyltrimethoxysilane (OTS). The resultant imprinted materials showed shape selectivity for the imprint molecules even though the monolayer of octadecyl groups is not rigid or even well defined (Fig. 14c and d). Size and shape selectivity of small organic molecules is clearly possible through grafted surface imprinting on PMS materials.

Synthesizing mesoporous (organo)silica with surface imprints

Post-synthetic grafting methods are certainly easy to use and modify, but this approach does suffer from one flaw in particular: grafted species can block pores or decrease their diameters significantly: in the previous example, the pore diameter went from 4.5 nm in the original PMS to 2.4 nm after OTS coating. This pore diameter decrease can have major implications for accessibility, which could defeat the purpose of using a mesoporous material altogether. The obvious alternative is building mesoporous (organo)silica with imprinted surface sites formed *in situ*. This strategy arguably makes better use of the mesoporous nature of

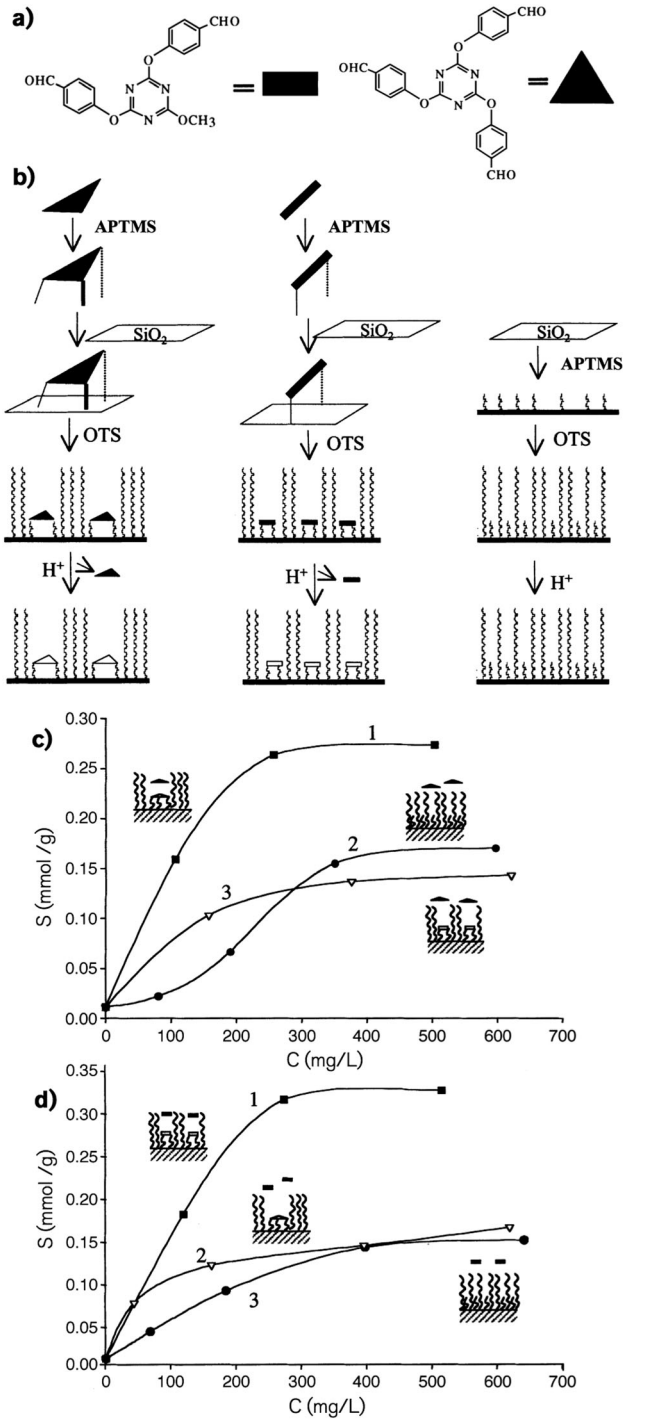

Fig. 14 (a) Structure of rectangular and triangular imprint molecules. (b) Schematic representation of imprint coating on SBA-15-type PMS with a pore diameter of 2.5 nm: grafting of the IC or APTMS, followed by residual silanol capping using either octadecyltrimethoxysilane (OTS) or trimethoxypropylsilane (TMPS). Triangular imprinting yields triangular cavities, rectangular imprinting yields linear cavities, and random APTMS grafting yields point cavities. (c) Specific adsorption S of triangular molecules on triangular (**1**), linear (**2**) and point (**3**) cavities. (d) Specific adsorption S of rectangular molecules on linear (**1**), triangular (**2**) and point (**3**) cavities. Reproduced with permission from ref. 99. Copyright 2000 Wiley VCH.

PMS/PMO because it does not introduce any additional species into the pore channels.

Taking a creative approach to synthesizing an IC, Johnson and coworkers reported template-directed surface molecular imprinting for the selective adsorption of 2,4,6-trinitrotoluene (TNT, **1**) (Fig. 15).[100] The mixed ethane- and diethylbenzene-bridged[101] PMO was templated using an oligomeric alkyl poly(ethylene oxide) surfactant, Brij-76 (**2**), as both the template and the functional monomer. The terminal alcohol (green) was reacted with 3,5-dinitrobenzoyl chloride to form an IC (**3**) containing a terminal 3,5-dinitrobenzoate group (fuchsia). Two crosslinkers were used: 1,4-bis(trimethoxysilylethyl)benzene (BTMEB, **4**) for its ability to interact noncovalently with the imprint functionality, and BTMA (**5**, trimethoxysilane analogue of **9**, Fig. 6a) for good structural integrity.[102] Using a variety of template/IC and BTMEB/BTMA ratios, a series of molecularly imprinted mesoporous organosilica (MIMO) materials were synthesized that displayed varying physicochemical and binding properties. When **3** comprised 12.5% of the total amount of template and when **4** comprised 30% of the crosslinker, the best compromise of structure, capacity, and selectivity was achieved in the MIMO. When the amount of **3** was increased in the template mixture, greater capacity but lower selectivity was observed. An increase in the amount of **4** resulted in both greater uptake capacity of TNT and better selectivity for it. However, when **4** comprised more than 40% of the total crosslinker, a transition from mesopores to micropores and a decrease in the overall pore order and uniformity were observed, likely due to the fact that this high loading of a non-rigid precursor weakens the structural integrity of the MIMO and its ability to hold the templated shape. In binding tests of TNT and structural analogues, binding equilibrium in static adsorption on the optimized MIMO was achieved in less than 3 minutes. By comparison, MIMOs with lower pore size and shape uniformity took longer to reach adsorption equilibrium (up to 30 minutes). This provides excellent evidence for the advantage of ordered mesopores over poorly ordered mesopores or micropores for rapid target binding, even when a surface imprinting method is used to allow for the easiest access possible to imprint sites. Additionally, this example highlights the balance that exists in optimizing different parameters in a MIP system: superior performance is not necessarily achieved with maximum loading of imprint sites.

An attractive feature of sol–gel silica is its high crosslink density, which gives it rigidity and the ability to form very fine features. Silica is not chiral, but because of its utility in so many separation and sensing applications (either as a solid support or an active material itself), significant interest exists in imbuing it with a chiral nature.[103] The Marx group has reported a chirally imprinted thin film of sol–gel organosilica (not containing templated mesopores) that displayed enantioselectivity through careful tailoring of the R′ groups on $(RO)_3SiR'$ precursors to match specific functionalities on a chosen imprint molecule.[104] In this case, an enantioselective negative chiral image was incorporated into imprint cavities through the spatial arrangement and orientation of organic functional monomers. However, this kind of chiral imprinting relies almost entirely on the presence of organic functional groups for enantioselectivity. To determine

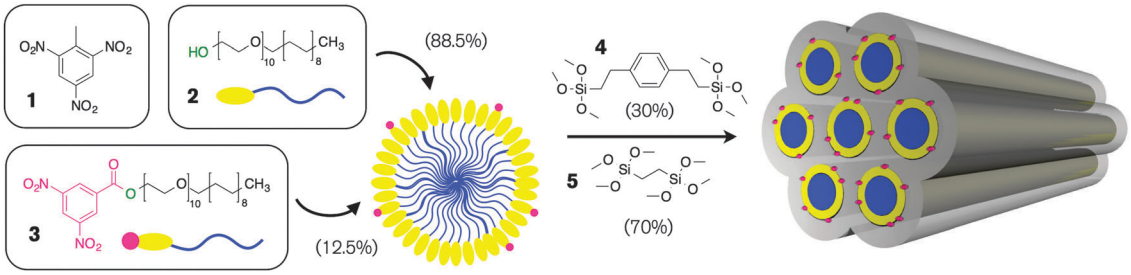

Fig. 15 Schematic representation of template-directed surface molecular imprinting of a PMO for selective adsorption of 2,4,6-trinitrotoluene (TNT, **1**) using Brij 76 (**2**) and dinitrobenzene-capped Brij 76 (**3**) as the template and IC, respectively. Template micelles with 12.5% **3** form in solution, and cooperatively self-assemble with two crosslinkers 1,4-bis(trimethoxysilylethyl)benzene (BTMEB, **4**) and bis(trimethoxysilyl)methane (BTMA, **5**) to form an optimized surface-imprinted PMO. Removal of the mixed surfactant template leaves surface imprint cavities. Adapted from ref. 100.

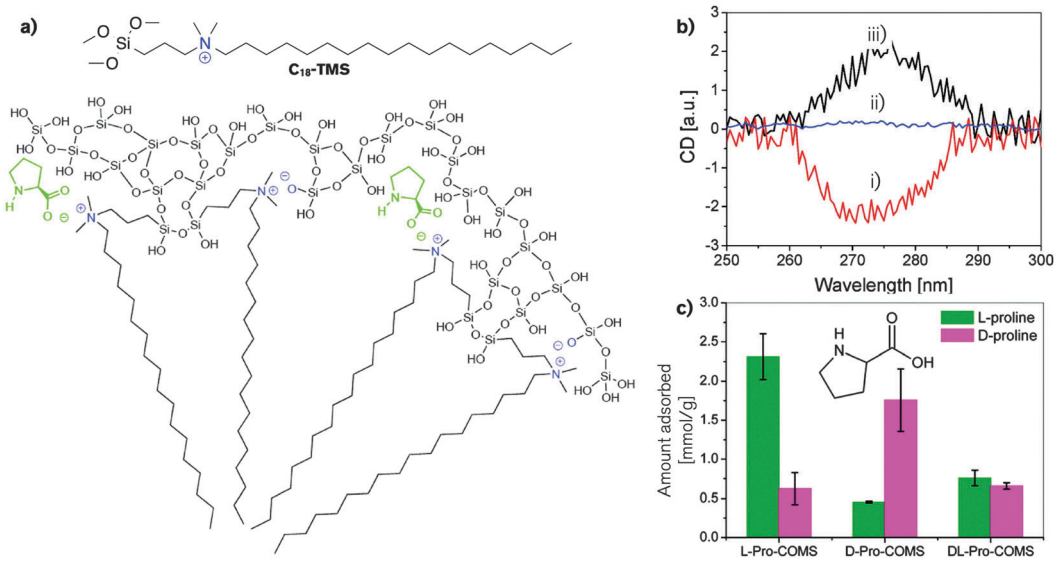

Fig. 16 (a) Structure of quaternized aminosilane C_{18}-TMS and schematic of micelle-pore wall structure, where C_{18}-TMS in dimers templates the pores and interacts with the chiral amino acid L-proline (green) to produce chiral surface imprint sites. (b) Solid-state induced circular dichroism (CD) of calcined mesoporous samples imprinted with (i) L-proline, (ii) DL-proline, and (iii) D-proline. Reproduced with permission from.[106] Copyright 2011 American Chemical Society. (c) Adsorption of L- and D-proline on calcined mesoporous materials imprinted with L-proline, D-proline, and DL-proline, showing selectivity for the imprinted enantiomer. Reproduced with permission from ref. 107. Copyright 2012 American Chemical Society.

exactly how finely featured silica can be, it is necessary to remove the organics and look at the purely inorganic matrix.

In MCM-41 synthesis, a common practice is to remove the template by calcination because the strong ionic interactions between the cationic surfactant template and the silica matrix make solvent extraction less reliable. Under typical calcination conditions (450 °C or higher, flowing air, oxygen, and/or nitrogen atmosphere), all organic fragments within a sample (template, R′ groups, residual OR groups) are burned away, and additional condensation often occurs.[105] The Coronas group made use of this to demonstrate the creation of chiral imprint cavities in calcined imprinted MCM-41.[106] As with the surface imprinting reported by Johnson (*vide supra*), the authors used a modified surfactant as the functional monomer. However, in this case, the quaternized aminosilane surfactant functional monomer was used exclusively as the pore template (no unmodified surfactant was used, Fig. 16a). The positively charged quaternary ammonium group interacted with the deprotonated form of the imprint amino acid (in this case, L- or D-proline) in basic media, and created imprint cavities on the surface of the pores. A control material imprinted with DL-proline (racemic mixture) was also prepared. The benefit to using an alkoxysilane-containing functional monomer of this type is that by virtue of its ability to participate in three interactions simultaneously (with the imprint, the crosslinker, and the template), it in effect guaranteed the precise placement of imprint cavities on the surface of the templated pores. Because the template was covalently bound to the mesoporous material by Si–C bonds, it was necessary to use calcination to vacate the pores. Confirmation of the presence of chiral sites after calcination was obtained by solid-state induced circular dichroism, which measures the asymmetry induced on an achiral molecule (in this case, phenol) by a chiral environment (Fig. 16b). The signals of the chiral imprinted materials are of the same intensity

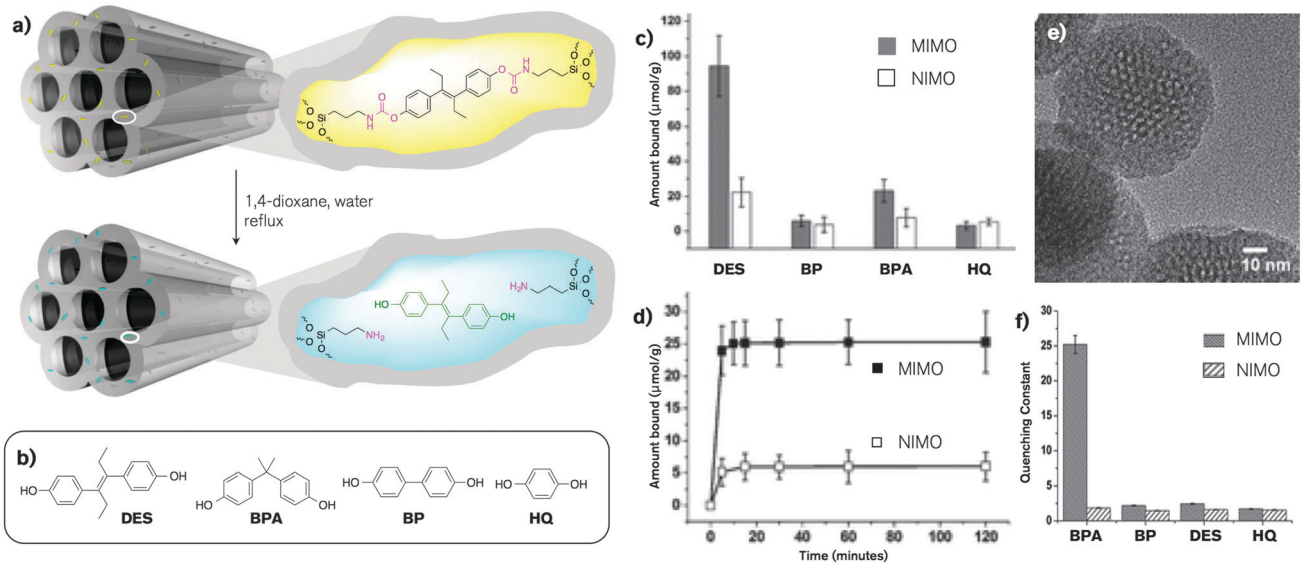

Fig. 17 (a) Schematic representation of imprinted PMO material before and after imprint removal, showing the carbamate bond used in sacrificial spacer imprinting (magenta) and the fit of the imprint molecule (green) inside the imprint cavity. (b) Molecular structures of analytes used static binding tests: diethylstilbestrol (**DEB**), bisphenol-A (**BPA**), 4,4′-biphenol (**BP**), and hydroquinone (**HQ**). (c) Static binding tests for four analytes using the imprinted PMO and a nonimprinted control PMO. (d) Kinetic binding profile for **DEB** of the imprinted PMO and the nonimprinted control. (e) Transmission electron micrographs of imprinted PMO showing the spherical shape and small particle size produced. From ref. 108. Reproduced by permission from the Royal Society of Chemistry. (f) Fluorescence quenching of CdSe quantum dots embedded in BPA-imprinted PMO and nonimprinted control as a way of detecting the binding of four analytes in solution. From ref. 110. Reproduced by permission from the Royal Society of Chemistry.

but opposite value (indicating opposite chiral handedness), while there is no observed signal for the DL-imprinted material. In a binding test using a racemic mixture of L- and D-proline, clear enantioselectivity was observed for both chiral materials, while the DL-imprinted material shows no preferential adsorption. (Fig. 16c).[107] Despite observed shrinkage in the silica matrix after calcination and the absence of organic functional groups, this work successfully demonstrated the generation of extremely fine imprint sites in pure sol–gel silica. Morrison's assertion in 1959 that silica shrinkage would necessarily destroy imprint sites[21] seems to have been conclusively proven incorrect.

Imprinting inside the walls of a mesoporous material

Achieving surface imprinting in PMOs is a relatively easy task when grafting is used, as there is no ambiguity as to the location of the imprint sites. Likewise, cocondensation with any $(RO)_3SiR'$ species will create a material with R′ on the pore surface, allowing very simple surface imprinting. *In situ* surface imprinting by cocondensation can also be controlled by exploiting strong template-functional monomer interactions to create "dents" in the pore walls, as discussed in the previous examples. Making the transition to imprinting *inside* the pore walls, however, is a less straightforward task. The main challenge is not producing a material with the correct chemical functionality; this is as straightforward as synthesizing an appropriate IC and cocondensing it with a given crosslinker in the presence of an appropriate template. The challenge is finding evidence that the imprint sites are indeed inside the walls of the material. If the IC is of the form $(RO)_3SiR'Si(OR)_3$, it is reasonable to predict that it will be integrated into the matrix of the pore walls. However, depending on the system, it is also possible that the IC will have favourable interactions with the template, and thus be located primarily on pore surfaces.

The Chang group were the first to report the synthesis of a MIMO (MCM-41-type) with the IC designed to create imprint sites inside the pore walls.[108] The imprint molecule, diethylstilbestrol (DES), was bound at two points to ICPTES *via* a carbamate linker (Fig. 17a).[109] The imprint molecule was one of four used in binding tests; the other three, bisphenol A (BPA), 4,4′-biphenol (BP), and hydroquinone (HQ), were chosen for their structural similarity but different phenol separation distances (Fig. 17b). Compared to a control nonimprinted mesoporous organosilica (NIMO) prepared with APTES instead of the IC, the MIMO showed large uptake capacity and selectivity for DES, while the control showed low capacity and little selectivity for all four targets (Fig. 17c). In a kinetic binding test using DES, the both the MIMO and NIMO reached 95% of equilibrium in approximately 5 minutes (the MIMO was slightly faster), and complete equilibrium in less than 10 minutes (Fig. 17d). This binding speed is close to that of surface-imprinted PMOs, which is reasonable given the very short diffusion distances in PMS/PMO materials. In the spherical particles produced in this report (Fig. 17e), the authors estimated the wall thickness to be 2.3 nm. Given the length of the DES molecule (1.4 nm), they reasoned that the imprint sites were most likely embedded in the walls of the imprinted PMO particles. However, in the absence of a binding test using a molecule with a larger size than DES, which could confirm a closed size-selective cavity, it is also possible that the imprint sites were on or only partially embedded in the surface of the pores. In a follow-up report, the

Chang group prepared a BPA-imprinted MCM-41-type PMO in which CdSe quantum dots were used to detect binding of targets by fluorescence quenching.[110] The imprinted PMO showed excellent binding for BPA but boor binding for the larger DES and smaller targets BP and HQ (Fig. 17f), which confirmed that a size-selective cavity had indeed been produced.

We recently reported the synthesis and characterization of SBA-15-type MIMO, where careful characterization of the porous structure of the material did indeed offer evidence of buried imprint sites.[111] Using bisphenol A (BPA) as an imprint molecule, the semicovalent imprinting strategy with ICPTES as the functional monomer shown in previous examples discussed here (IC formed by a carbamate bond) and TEOS as the cross-linker, we prepared a series of three SBA-15-type materials: MIMO (**I**) containing the imprint molecule, a control non-imprinted mesoporous organosilica (NIMO, **II**) prepared with ICPTES (which was reduced to a primary amine during the synthesis) and no BPA, and control blank SBA-15 (**III**), synthesized from only TEOS (Fig. 18a). Based on careful assessment of the porous structure (pore volume, pore diameter, and wall thickness) found by gas sorption and small-angle X-ray scattering, and the likely interactions that the molecular precursors had with the pore template, we concluded that the imprint cavities in **I** were most likely embedded in the pore walls, the 3-aminopropyl groups in **II** were on the surface of the pores, and **III** contained the typical surface silanol and residual ethoxy groups found in this class of materials, which allowed it to demonstrate the effect of nonspecific binding only. In solid-phase extraction tests (flow rate $\sim$0.5 mL min^{-1}) of four competing targets in aqueous solution (phenol (P), resorcinol (R), 4,4′-biphenol (BP), and bisphenol A (BPA), Fig. 18b), a clear imprinting effect was observed (Fig. 18c). Both BP and BPA were strongly bound in **I**, while P and R, which are significantly smaller, could not participate in interactions with both amines in the imprint cavities. Some weak binding of BP and BPA was shown in both **II** and **III**, but the rinse step removed most of the bound molecules. Despite the absence of imprint functional groups, **III** showed similar binding behaviour to **II**, which, coupled with the strong binding observed for **I**, confirms the creation of imprint cavities with precisely arranged primary amine groups. Static binding of the large dye bromothymol blue (BTB) served to confirm that **I** contained imprint cavities that were fairly size selective (Fig. 18d). **II** bound 98% of the dye, while **I** only bound 71%. Approximately 30% of the amount could be accounted for by nonspecific binding (as found from the dye bound to **III**). Overall the results confirmed that the easily accessible surface amines in **II** were different from the at least partially buried amines in the imprint cavities of **I**. In a porous material with walls less than 5 nm thick, the depth at which imprint cavities are buried is likely not sufficient to completely exclude bulkier molecules like BTB, which still contains the same spatial arrangement and separation of the phenol groups.

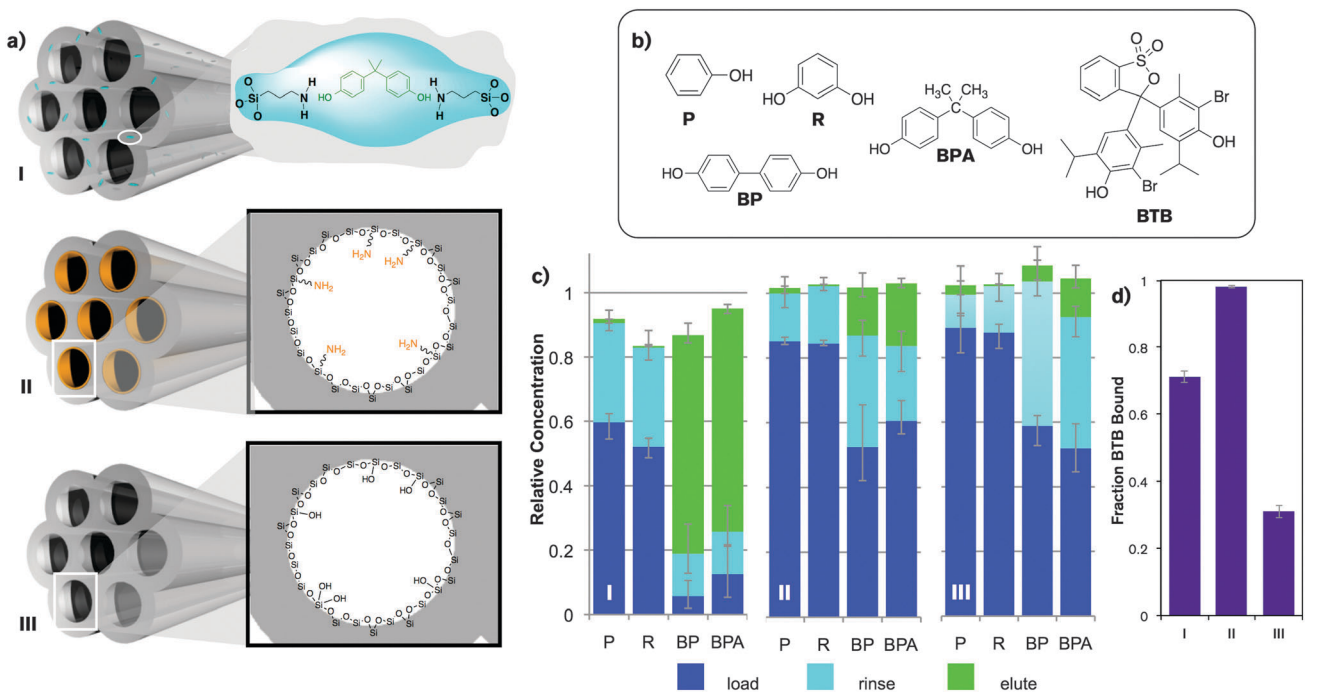

Fig. 18 Molecular imprinting of bisphenol A in mesoporous SBA-15-type organosilica. (a) Schematic representation of the functional groups present in MIMO with embedded imprint cavities after imprint removal (**I**), non-imprinted mesoporous organosilica with 3-aminopropyl groups on the pore surface (**II**), and control SBA-15 with surface silanols (**III**) and some residual ethoxy groups (not shown). (b) Structures of analyte molecules used: phenol (P), resorcinol (R), 4,4′-biphenol (BP), bisphenol A (BPA, imprint molecule), and bromothymol blue (BTB). (c) Stacked solid-phase extraction plots of a mixed aqueous solution of P, R, BP, and BPA (each at a concentration of 1×10^{-4} M). (d) Fraction of BTB bound to **I**, **II**, and **III** in static binding, found by the absorbance at 615 nm of the solution relative to the stock solution of BTB. Reproduced with permission from.[111] Copyright 2011 American Chemical Society.

These two examples served as the first confirmation that successful molecular imprinting inside the walls of the two most commonly used classes of PMS materials (MCM-41 and SBA-15) was possible. As opposed to surface imprinting techniques, wall-imprinting has the potential to produce MIMO materials with a high degree of size and shape selectivity that is similar to imprinting in bulk MIO materials, but still show the very fast kinetic binding profiles made possible by templated mesopores.

Outlook for imprinting in silica

Clear advantages have been demonstrated moving from bulk monoliths to particles to thin films to templated mesoporous materials. The importance of diffusion length for target binding in an imprinted material is evident in kinetic binding behaviour, and an obvious improvement exists when controlled porosity in the form of uniform channels is created. Three years ago we asked ourselves the question: why PMO?[112] Molecular imprinting imbues any polymer with tremendous functionality and utility, and the intersection of the fields of molecular imprinting and supramolecular pore templating offers a truly elegant answer to this question.

The extensive library of molecular sol–gel precursors that are commercially available makes careful tuning of the imprinting method is easy. The wide range of processing conditions that are possible with sol–gel chemistry (including non-aqueous methods) make virtually any imprinting system possible: noncovalent, semi-covalent, ionic, and coordination imprinting have all been successfully achieved in silica, and it is likely that covalent imprinting has been overlooked so far simply because of the energetic cost of binding a target relative to the semicovalent approach. The ease with which the morphology of sol–gel materials can be controlled gives them a significant advantage over many organic polymer systems used for molecular imprinting, and allows for fine control over diffusion distances down to the nanometre scale. Finally, the development of hierarchical imprinting/templating approaches in highly porous MIMO materials, both surface- and wall-imprinted, opens the door to the production of imprinted materials that possess excellent starting material economy from the first step of synthesis to the final imprinted material, a greener chemical system that uses water and alcohol instead of toxic organic solvents, and the ability to exploit virtually all of the successes of more than eight decades of molecular imprinting and four decades of sol–gel science and technology.

It is certain that imprinting in organic and inorganic polymers will continue to travel parallel paths. However, the renaissance of imprinted silica and the birth of imprinted mesoporous organosilica have demonstrated silica's excellence as not just the passive solid support used throughout the organic polymer field, but a truly imprinted polymer matrix, able to resolve fine molecular detail through delicate selectivity and tremendous versatility.

Notes and references

1 Z.-H. Meng, Molecularly Imprinted Sol-Gel Sensors, in *Molecularly Imprinted Sensors: Overview and Applications*, ed. S. Li, Y. Ge, S. A. Piletsky and J. Lunec, Elsevier, Amsterdam, 2012, pp. 303–337.
2 A. Walcarius and M. Collinson, *Annu. Rev. Anal. Chem.*, 2009, **2**, 121–143.
3 M. Díaz-García and R. Laíño, *Microchim. Acta*, 2005, **149**, 19–36.
4 M. E. Davis, *Stud. Surf. Sci. Catal.*, 2000, **130A**, 49–59.
5 D. Y. Sasaki, *Tech. Instrum. Anal. Chem.*, 2000, **23**, 213–244.
6 M. M. Collinson, Imprinted Functionalized Silica, in *The Supramolecular Chemistry of Organic-Inorganic Hybrid Materials*, ed. K. Rurack and R. Martínez-Máñez, John Wiley & Sons, Hoboken, 2010, pp. 581–598.
7 MIP Database. http://mipdatabase.com/Database.html, accessed 14 May 2013.
8 L. Chen, S. Xu and J. Li, *Chem. Soc. Rev.*, 2011, **40**, 2922–2942 and references therein.
9 C. Alexander, H. S. Andersson, L. I. Andersson, R. J. Ansell, N. Kirsch, I. A. Nicholls, J. O'mahony and M. J. Whitcombe, *J. Mol. Recognit.*, 2006, **19**, 106–180 and references therein.
10 B. Sellergren and C. Allender, *Adv. Drug Delivery Rev.*, 2005, **57**, 1733–1741 and references therein.
11 A. Mayes and M. Whitcombe, *Adv. Drug Delivery Rev.*, 2005, **57**, 1742–1778 and references therein.
12 H. S. Andersson and I. A. Nicholls, *Tech. Instrum. Anal. Chem.*, 2000, **23**, 1–19 and references therein.
13 M. V. Polyakov, *Zh. Fiz. Khim.*, 1931, **2**, 799–805.
14 L. Pauling, *J. Am. Chem. Soc.*, 1940, **62**, 2643–2657.
15 L. Pauling and D. Campbell, *J. Exp. Med.*, 1942, **76**, 211–220.
16 P. Ehrlich, *Studies on Immunity*, John Wiley and Sons, New York, 1906.
17 L. Pauling, D. H. Campbell and D. Pressman, *Physiol. Rev.*, 1943, **23**, 203–219.
18 F. H. Dickey, *Proc. Natl. Acad. Sci. U. S. A.*, 1949, **35**, 227–229.
19 F. H. Dickey, *J. Phys. Chem.*, 1955, **59**, 695–707.
20 R. G. Haldeman and P. H. Emmett, *J. Phys. Chem.*, 1955, **59**, 1039–1043.
21 J. L. Morrison, M. Worsley, D. R. Shaw and G. W. Hodgson, *Can. J. Chem.*, 1959, **37**, 1986–1995.
22 G. Wulff and A. Sarhan, *Angew. Chem., Int. Ed. Engl.*, 1972, **11**, 341.
23 T. Takagishi and I. M. Klotz, *Biopolymers*, 1972, **11**, 483–491.
24 G. Wulff, *Angew. Chem., Int. Ed.*, 1995, **34**, 1812–1832.
25 K. Mosbach, *Trends Biochem. Sci.*, 1994, **19**, 9–14.
26 O. Ramstrom, I. A. Nicholls and K. Mosbach, *Tetrahedron: Asymmetry*, 1994, **5**, 649–656.
27 Y. Tominaga, T. Kubo, K. Kaya and K. Hosoya, *Macromolecules*, 2009, **42**, 2911–2915.
28 S. McNiven, Y. Yokobayashi, S. H. Cheong and I. Karube, *Chem. Lett.*, 1997, 1297–1298.
29 G. Wulff, W. Vesper, R. Grobeeinsler and A. Sarhan, *Makromol. Chem.*, 1977, **178**, 2799–2816.
30 K. J. Shea and T. K. Dougherty, *J. Am. Chem. Soc.*, 1986, **108**, 1091–1093.

31 G. Wulff, W. Best and A. Akelah, *React. Polym.*, 1984, **2**, 167–174.
32 M. Whitcombe, M. Rodriguez, P. Villar and E. Vulfson, *J. Am. Chem. Soc.*, 1995, **117**, 7105–7111.
33 Y. Fujii, K. Matsutani and K. Kikuchi, *J. Chem. Soc., Chem. Commun.*, 1985, 415–417.
34 M. Burleigh, S. Dai, C. Barnes and Z. Xue, *Sep. Sci. Technol.*, 2001, **36**, 3395–3409.
35 T. Alizadeh, *Anal. Chim. Acta*, 2008, **623**, 101–108.
36 D. A. Spivak, Selectivity in Molecularly Imprinted Polymers, in *Molecularly Imprinted Materials: Science and Technology*, ed. O. Ramström and M. Yan, Marcel Dekker, New York, 2005, pp. 395–417.
37 D. Spivak, M. A. Gilmore and K. J. Shea, Evaluation of Binding and Origins of Specificity of 9-Ethyladenine Imprinted Polymers, *J. Am. Chem. Soc.*, 1997, **119**, 4388–4393.
38 D. Spivak, *Adv. Drug Delivery Rev.*, 2005, **57**, 1779–1794.
39 B. L. Roth, E. Lopez, S. Patel and W. K. Kroeze, *Neuroscientist*, 2000, **6**, 252–262.
40 D. Avnir, *Acc. Chem. Res.*, 1995, **28**, 328–334.
41 H. Schmidt, H. Scholze and A. Kaiser, *J. Non-Cryst. Solids*, 1984, **63**, 1–11.
42 H. Schmidt, *J. Non-Cryst. Solids*, 1985, **73**, 681–691.
43 C. J. Brinker and G. W. Scherer, Hydrolysis and Condensation II: Silicates, *Sol-Gel Science: The Physics and Chemistry of Sol-Gel Processing*, Academic Press, San Diego, 1990, pp. 97–234.
44 R. Wang, U. Narang, P. N. Prasad and F. V. Bright, *Anal. Chem.*, 1993, **65**, 2671–2675.
45 M. A. Doody, G. A. Baker, S. Pandey and F. V. Bright, *Chem. Mater.*, 2000, **12**, 1142–1147.
46 In most cases, $m = 3$.
47 O. Ramström and M. Yan, Molecular Imprint – An Introduction, in *Molecularly Imprinted Materials: Science and Technology*, ed. O. Ramström and M. Yan, Marcel Dekker, New York, 2005, pp. 1–12.
48 A. Katz and M. E. Davis, *Nature*, 2000, **403**, 286–289.
49 The amine protecting group *N-tert*-butoxycarbonyl (*t*BOC) used in organic synthesis is a carbamate bond with primary and secondary amines.
50 N. Pérez-Moral and A. G. Mayes, MIP Formats for Analytical Applications, in *Molecular Imprinting of Polymers*, ed. S. Piletsky and A. Turner, Landes Bioscience, Georgetown, 2006, pp. 1–11.
51 W. Stöber, A. Fink and E. Bohn, *J. Colloid Interface Sci.*, 1968, **26**, 62–69.
52 K. Hartlen, A. Athanasopoulos and V. Kitaev, *Langmuir*, 2008, **24**, 1714–1720.
53 K. Suzuki, S. Sato and M. Fujita, *Nat. Chem.*, 2009, **2**, 25–29.
54 C. Ki, C. Oh, S.-G. Oh and J. Chang, *J. Am. Chem. Soc.*, 2002, **124**, 14838–14839.
55 C. J. Brinker and G. W. Scherer, Film Formation, *Sol-Gel Science: The Physics and Chemistry of Sol-Gel Processing*, Academic Press, San Diego, 1990, pp. 787–838.
56 R. Makote and M. Collinson, *Chem. Mater.*, 1998, **10**, 2440–2445.
57 S. Lowell, J. E. Shields, M. A. Thomas and M. Thommes, *Characterization of Porous Solids and Powders: Surface Area, Pore Size and Density*, Kluwer Academic Publishers, Dordrecht, 1st edn, 2004.
58 W. Wang, D. Grozea, A. Kim, D. Perovic and G. Ozin, *Adv. Mater.*, 2010, **22**, 99–102.
59 Ellipsometric porosimetry (EP) is performed with water vapour, and the treatment of raw data to determine porosity features involves the contact angle of water on the given material. Contact angles are generally measured on a bulk surface, and it is debatable whether this contact angle is valid on the nanometre scale. Also, when films are hydrophobic, this causes challenges for water adsorption in very small pores.
60 S. Marx and Z. Liron, *Chem. Mater.*, 2001, **13**, 3624–3630.
61 E. L. Shughart, K. Ahsan, M. R. Detty and F. V. Bright, *Anal. Chem.*, 2006, **78**, 3165–3170.
62 S. Satoh, I. Matsuyama and K. Susa, *J. Non-Cryst. Solids*, 1995, **190**, 206–211.
63 C. McDonagh, P. Bowe, K. Mongey and B. D. MacCraith, *J. Non-Cryst. Solids*, 2002, **306**, 138–148.
64 J. Rouquerol, D. Avnir, C. Fairbridge, D. Everett, J. Haynes, N. Pernicone, J. Ramsay, K. Sing and K. Unger, *Pure Appl. Chem.*, 1994, **66**, 1739–1758.
65 C. Kresge, M. Leonowicz, W. Roth, J. Vartuli and J. Beck, *Nature*, 1992, **359**, 710–712.
66 D. Zhao, J. Feng, Q. Huo, N. Melosh, G. Fredrickson, B. Chmelka and G. Stucky, *Science*, 1998, **279**, 548–552.
67 T. Asefa, M. MacLachlan, N. Coombs and G. Ozin, *Nature*, 1999, **402**, 867–871.
68 B. Melde, B. Holland, C. Blanford and A. Stein, *Chem. Mater.*, 1999, **11**, 3302–3308.
69 S. Inagaki, S. Guan, Y. Fukushima, T. Ohsuna and O. Terasaki, *J. Am. Chem. Soc.*, 1999, **121**, 9611–9614.
70 F. Schuth, *Stud. Surf. Sci. Catal.*, 2004, **148**, 1–13.
71 A. Taguchi and F. Schüth, *Microporous Mesoporous Mater.*, 2005, **77**, 1–45.
72 W. J. Hunks and G. A. Ozin, *J. Mater. Chem.*, 2005, **15**, 3716.
73 B. Hatton, K. Landskron, W. Whitnall, D. Perovic and G. Ozin, *Acc. Chem. Res.*, 2005, **38**, 305–312.
74 F. Hoffmann, M. Cornelius, J. Morell and M. Fröba, *Angew. Chem., Int. Ed.*, 2006, **45**, 3216–3251.
75 M. Vallet-Regí, F. Balas and D. Arcos, *Angew. Chem., Int. Ed.*, 2007, **46**, 7548–7558.
76 Y. Wan and D. Zhao, *Chem. Rev.*, 2007, **107**, 2821–2860 and references therein.
77 S. Shylesh, P. P. Samuel, S. Sisodiya and A. P. Singh, *Catal. Surv. Asia*, 2008, **12**, 266–282.
78 L. D. Bonifacio, B. V. Lotsch and G. A. Ozin, Periodic Mesoporous Materials: Holes Filled with Opportunities, in *Comprehensive Nanoscience and Technology*, ed. D. L. Andrews, G. D. Scholes and G. P. Wiederrecht, Academic Press, Amsterdam, 2010, vol. 5, pp. 69–125.

79 A. Walcarius and L. Mercier, *J. Mater. Chem.*, 2010, **20**, 4478–4511.
80 N. Mizoshita, T. Tani and S. Inagaki, *Chem. Soc. Rev.*, 2011, **40**, 789.
81 F. Hoffmann and M. Fröba, *Chem. Soc. Rev.*, 2011, **40**, 608.
82 M. C. Orilall and U. Wiesner, *Chem. Soc. Rev.*, 2011, **40**, 520.
83 G. J. A. A. Soler-Illia and O. Azzaroni, *Chem. Soc. Rev.*, 2011, **40**, 1107.
84 Y. Han and D. Zhang, *Curr. Opin. Chem. Eng.*, 2012, **1**, 129–137.
85 T. Asefa and Z. Tao, *Can. J. Chem.*, 2012, **90**, 1015–1031.
86 E.-B. Cho, D. Kim and M. Jaroniec, *Langmuir*, 2007, **23**, 11844–11849.
87 S. Qiao, C. Lin, Y. Jin, Z. Li, Z. Yan, Z. Hao, Y. Huang and G. Lu, *J. Phys. Chem. C*, 2009, **113**, 8673–8682.
88 P. Mohanty and K. Landskron, *Nanoscale Res. Lett.*, 2009, **4**, 169–172.
89 E.-B. Cho, D. Kim and M. Jaroniec, *J. Phys. Chem. C*, 2008, **112**, 4897–4902.
90 B. Hatton, K. Landskron, W. Whitnall, D. Perovic and G. Ozin, *Adv. Funct. Mater.*, 2005, **15**, 823–829.
91 S. Park and C.-S. Ha, *Chem. Mater.*, 2005, **17**, 3519–3523.
92 L. Mercier and T. J. Pinnavaia, *Adv. Mater.*, 1997, **9**, 500–503.
93 Q. Huo, D. Margolese, U. Ciesla, D. Demuth, P. Feng, T. Gier, P. Sieger, A. Firouzi, B. Chmelka and F. Schüth, *et al.*, *Chem. Mater.*, 1994, **6**, 1176–1191.
94 Q. Huo, D. I. Margolese, U. Ciesla, P. Feng, T. E. Gier, P. Sieger, R. Leon, P. M. Petroff, F. Schuth and G. D. Stucky, *Nature*, 1994, **368**, 317–321.
95 X. Feng, *Science*, 1997, **276**, 923–926.
96 J. Liu, X. Feng, G. E. Fryxell, L.-Q. Wang, A. Y. Kim and M. Gong, *Adv. Mater.*, 1998, **10**, 161–165.
97 S. Dai, M. Burleigh, Y. Shin, C. Morrow, C. Barnes and Z. Xue, *Angew. Chem., Int. Ed.*, 1999, **38**, 1235–1239.
98 S. Dai, *Chem.–Eur. J.*, 2001, **7**, 763–768.
99 Y. Shin, J. Liu, L. Q. Wang, Z. Nie, W. D. Samuels, G. E. Fryxell and G. J. Exarhos, *Angew. Chem., Int. Ed.*, 2000, **39**, 2702–2707.
100 B. Johnson, B. Melde, P. Charles, D. Cardona, M. Dinderman, A. Malanoski and S. Qadri, *Langmuir*, 2008, **24**, 9024–9029.
101 The term ''bridged'' here is used with the parent name of the organic fragment R′ that joins two $Si(OR)_3$ groups in a silsesquioxane organosilica precursor molecule. It is common to call PMO synthesized from BTEA ''ethane PMO'' or ''ethane-bridged PMO''.
102 The less rigid the organic linker in a silsesquioxane PMO precursor, the poorer the structural integrity of the PMO after template removal. PMOs made from precursors containing propyl or longer flexible groups collapse upon template removal. A mixed precursor approach can circumvent this problem.
103 S. Marx and D. Avnir, *Acc. Chem. Res.*, 2007, **40**, 768–776.
104 S. Fireman-Shoresh, D. Avnir and S. Marx, *Chem. Mater.*, 2003, **15**, 3607–3613.
105 F. Kleitz, W. Schmidt and F. Schüth, *Microporous Mesoporous Mater.*, 2003, **65**, 1–29.
106 S. Lacasta, V. Sebastián, C. Casado, A. Mayoral, P. Romero, A. Larrea, E. Vispe, P. López-Ram-de-Viu, S. Uriel and J. Coronas, *Chem. Mater.*, 2011, **23**, 1280–1287.
107 C. Casado, J. Castán, I. Gracia, M. Yus, A. Mayoral, V. Sebastián, P. López-Ram-de-Viu, S. Uriel and J. Coronas, *Langmuir*, 2012, **28**, 6638–6644.
108 B. Jung, M. Kim, W. Kim and J. Chang, *Chem. Commun.*, 2010, **46**, 3699–3701.
109 No doubt the popularity of the carbamate bond for semicovalent imprinting in sol–gel silica is caused at least in part by the early success it enjoyed, and a desire to introduce as few uncertain variables into a new imprinting system as possible. The carbamate is easy to form in excellent yield, and just as easily liberates a hydrogen bonding 3-aminopropane functionality. The prevalence of this bond in silica imprinting is akin to the extensive use of propranolol as an imprint molecule in noncovalently imprinted organic polymers, simply because it has come to be an archetypal imprint molecule.
110 Y. Kim, J. B. Jeon and J. Y. Chang, *J. Mater. Chem.*, 2012, **22**, 24075.
111 J. E. Lofgreen, I. Moudrakovski and G. Ozin, *ACS Nano*, 2011, **5**, 2277–2287.
112 W. Wang, J. E. Lofgreen and G. A. Ozin, *Small*, 2010, **6**, 2634–2642.